Multiple evidence for methylotrophic methanogenesis as the dominant methanogenic pathway in hypersaline sediments from the Orca Basin, Gulf of Mexico

Guang-Chao Zhuang [a,b,*,1], Felix J. Elling [a,*,1,2], Lisa M. Nigro [c], Vladimir Samarkin [b], Samantha B. Joye [b], Andreas Teske [c], Kai-Uwe Hinrichs [a]

[a] *Organic Geochemistry Group, MARUM Center for Marine Environmental Sciences, University of Bremen, 28359 Bremen, Germany*
[b] *Department of Marine Sciences, University of Georgia, 30602 Athens, GA, USA*
[c] *Department of Marine Sciences, University of North Carolina at Chapel Hill, Chapel Hill, 27599 NC, USA*

Received 11 December 2015; accepted in revised form 3 May 2016; available online 9 May 2016

Abstract

Among the most extreme habitats on Earth, dark, deep, anoxic brines host unique microbial ecosystems that remain largely unexplored. As the terminal step of anaerobic degradation of organic matter, methanogenesis is a potentially significant but poorly constrained process in deep-sea hypersaline environments. We combined biogeochemical and phylogenetic analyses with incubation experiments to unravel the origin of methane in the hypersaline sediments of Orca Basin in the northern Gulf of Mexico. Substantial concentrations of methane, up to 3.4 mM, coexisted with high concentrations of sulfate from 16 to 43 mM in two sediment cores retrieved from the northern and southern parts of Orca Basin. The strong depletion of ^{13}C in methane (−77‰ to −89‰) points towards a biological source. While low concentrations of competitive substrates limited the significance of hydrogenotrophic and acetoclastic methanogenesis, the presence of non-competitive methylated substrates (methanol, trimethylamine, dimethyl sulfide, dimethylsulfoniopropionate) supported the potential for methane generation through methylotrophic methanogenesis. Thermodynamic calculations demonstrated that hydrogenotrophic and acetoclastic methanogenesis were unlikely to occur under *in situ* conditions, while methylotrophic methanogenesis from a variety of substrates was highly favorable. Likewise, carbon isotope relationships between methylated substrates and methane suggested methylotrophic methanogenesis was the major source of methane. Stable and radio-isotope tracer experiments with ^{13}C-labeled bicarbonate, acetate and methanol and ^{14}C-labeled methylamine indicated that methylotrophic methanogenesis was the predominant methanogenic pathway. Based on 16S rRNA gene sequences, halophilic methylotrophic methanogens related to the genus *Methanohalophilus* dominated the benthic archaeal community in the northern basin and also occurred in the southern basin. High abundances of methanogen lipid biomarkers such as intact polar and polyunsaturated hydroxyarchaeols were detected in sediments from the northern basin, with lower abundances in the southern basin. Strong ^{13}C-depletion of saturated and monounsaturated hydroxyarchaeol were consistent with methylotrophic methanogenesis as the major methanogenic pathway. Collectively, the availability of methylated substrates, thermodynamic calculations,

* Corresponding authors at: Organic Geochemistry Group, MARUM Center for Marine Environmental Sciences, University of Bremen, 28359 Bremen, Germany (G.-C. Zhuang and F.J. Elling).
E-mail addresses: gzhuang@uga.edu (G.-C. Zhuang), felix_elling@fas.harvard.edu (F.J. Elling).
[1] These authors contributed equally to this work.
[2] Present address: Department of Earth and Planetary Sciences, Harvard University, Cambridge, MA 02138, USA.

http://dx.doi.org/10.1016/j.gca.2016.05.005

experimentally determined methanogenic activity as well as lipid and gene biomarkers support the hypothesis that methylotrophic methanogenesis is the predominant pathway of methane formation in the presence of sulfate in Orca Basin sediments.
Published by Elsevier Ltd.

Keywords: Methylotrophic methanogenesis; Methylated compounds; Lipids; Hypersaline sediment

1. INTRODUCTION

Hypersaline environments, defined as those with salinities exceeding 50‰, are widespread on Earth in settings such as coastal salt marshes and sabkhas, inland salt lakes, and deep-sea brine pools (Boetius and Joye, 2009; McGenity, 2010). Among the most extreme habitats on Earth, dark and anoxic seafloor brine lakes are known discovered in the deep sea of the Gulf of Mexico, the Mediterranean Sea, and the Red Sea, and are characterized by extremely high salinity, strong stratification, and steep geochemical gradients (Joye et al., 2005; Antunes et al., 2011). As halophiles are among the candidates for the earliest life forms on Earth, studying the microbial ecology of brine ecosystems may yield insights into the origins, metabolisms and limits of early microbial life on Earth and potentially other planets (Mancinelli et al., 2004). Despite harsh conditions, a diversity of microorganisms involved in fundamental biogeochemical processes, e.g., cycling of methane and sulfur, potentially support microbial ecosystems in these chemically distinct habitats (Joye et al., 2009). In particular, biological production of methane is proposed to play a key role in supporting carbon cycling in deep-sea brines and underlying sediments (Charlou et al., 2003; van der Wielen et al., 2005; Lazar et al., 2011).

Production of methane by methanogenic archaea is one of the terminal steps in organic matter degradation in anoxic environments. Methanogenic pathways are commonly classified with respect to the type of carbon source, i.e., CO_2 reduction by available hydrogen (hydrogenotrophic methanogenesis), acetate disproportionation (acetoclastic methanogenesis) and methanogenesis from methylated substrates, such as methanol, methylamines, and methyl sulfides (methylotrophic methanogenesis). Thermodynamically, methanogens are out-competed for hydrogen and acetate by sulfate reducers, and methane formation via these 'competitive' substrates is generally inhibited until sulfate is depleted. However, in the presence of sulfate, methanogens may circumvent competition by utilizing 'non-competitive' methylated substrates, as these are consumed exclusively or preferentially by methylotrophic methanogens (Oremland et al., 1982b). The stable carbon isotopic composition of methane has been used extensively for identifying its formation pathways in the environment (Whiticar et al., 1986; Whiticar, 1999; Conrad, 2005). Thermogenic generation of methane at high temperatures yields methane with $\delta^{13}C$ values $\sim -50‰$. In contrast, strong fractionation during biogenic methanogenesis leads to isotopically lighter methane, e.g., acetoclastic methanogenesis produces methane with $\delta^{13}C$ values in the range of $-70‰$ to $-50‰$ while hydrogenotrophic methanogenesis yields $\delta^{13}C$ values of $-110‰$ to $-60‰$ (Whiticar, 1999). Although little is known about the isotopic composition of methane derived from methylotrophic methanogenesis in the environment, large carbon isotope fractionation between methanol or trimethylamine and methane in pure cultures suggests that methane produced from these substrates should be similarly depleted as those produced from acetoclastic or hydrogenotrophic methanogenesis (Rosenfeld and Silverman, 1959; Summons et al., 1998; Londry et al., 2008; Penger et al., 2012).

In hypersaline environments, methylotrophic methanogenesis is considered to be of greater importance because of the high concentrations of sulfate found in these environments and the abundance of potential methylated substrates and their precursors (McGenity, 2010). Methylated substrates derive from organic matter decomposition, such as methanol derived from lignin and pectin degradation (Donnelly and Dagley, 1980; Schink and Zeikus, 1980). Methylamines and dimethyl sulfide (DMS) are also derived from the breakdown of osmolytes, e.g., glycine betaine and dimethylsulfoniopropionate (DMSP), which are ubiquitously synthesized by phytoplankton and by microbes inhabiting hypersaline environments (Oren, 1990; Zhuang et al., 2011). Since methanogens inhabiting hypersaline environments need to divert more energy for the biosynthesis or uptake of compatible solutes, methylotrophic methanogenesis might be more favorable than acetoclastic and hydrogenotrophic methanogenesis due to its higher energy yield (Oren, 1999; Roberts, 2005; McGenity, 2010). Although this hypothesis was proposed decades ago and supported by sparse *in vitro* methanogenic activity measurements and molecular analyses in hypersaline environments (Orphan et al., 2008; Smith et al., 2008; Lazar et al., 2011), to our knowledge, very limited information was available on the *in situ* abundance of methylated substrates, impeding our understanding of the relative importance of methylotrophic methanogenesis. In addition, geochemical and microbiological investigations of deep-sea brines mostly focused on the brine-seawater interface while benthic microbial communities and the processes associated with them remain largely unconstrained.

In this study, we sought to constrain methanogenic pathways by combining geochemical, physiological, and microbiological analyses of hypersaline sediments from Orca Basin, which contains the largest seafloor brine pool in the Gulf of Mexico covering approximately 200 km^2 (Pilcher and Blumstein, 2007). Natural abundances of major competitive and non-competitive substrates, stable carbon isotope compositions of methane and precursors, methanogenic activity with stable isotope tracer and radiotracers as well as methanogen lipid biomarkers and 16S

rRNA genes were comprehensively characterized to decipher the origin of methane in Orca Basin. The relationships between available substrates, methanogenic activity and methanogen populations provided new insights into the relative importance of different methanogenic pathways in deep-marine hypersaline sediments, in particular from non-competitive substrates.

2. MATERIALS AND METHODS

All geochemical data of this study are stored in the Pangaea database and are accessible via http://doi.pangaea.de/10.1594/PANGAEA.859443. Sequences were deposited at NCBI Genbank with accession numbers KP204602 to KP204835.

2.1. Site description and sampling

Orca Basin, a 25 km long, 15 km wide and 2400 m deep depression on the continental slope of the northern Gulf of Mexico, host a 200 m thick anoxic hypersaline brine at the basin bottom (Fig. 1; Shokes et al., 1977). Sediment samples were collected using a multicorer during expedition AT18-2 of the research vessel *R/V Atlantis*, in November 2010. Three multicores (60 cm) were recovered from the southern sub-basin (MUC-6, N 26.9080°, W 91.3348°, water depth: 2432 m), the northern sub-basin (MUC-7, N 27.0000°, W 91.2832°, water depth: 2339 m), and a non-brine 'reference site' (N 27.1235°, W 90.2878°, water depth: 2068 m) along the Louisiana-Texas continental slope, respectively (Fig. 1). Due to over-penetration of the multicore, the exact depth below seafloor is unknown for these cores but it is unlikely that over-penetration exceeded 10 cm. Sediment cores were transferred to a cold room after retrieval and sectioned at 4 °C (for sulfate, chloride, dissolved inorganic carbon, and rate measurement samples) or at room temperature (for all other geochemical parameters as well as lipid and gene analysis samples) within 12 h using a core extruder. Samples for methane concentration and isotope analysis (5 mL of sediment) were transferred into a 30 mL serum vial containing 2 mL of 1 M NaOH with a cut-off syringe, crimp-capped immediately, and

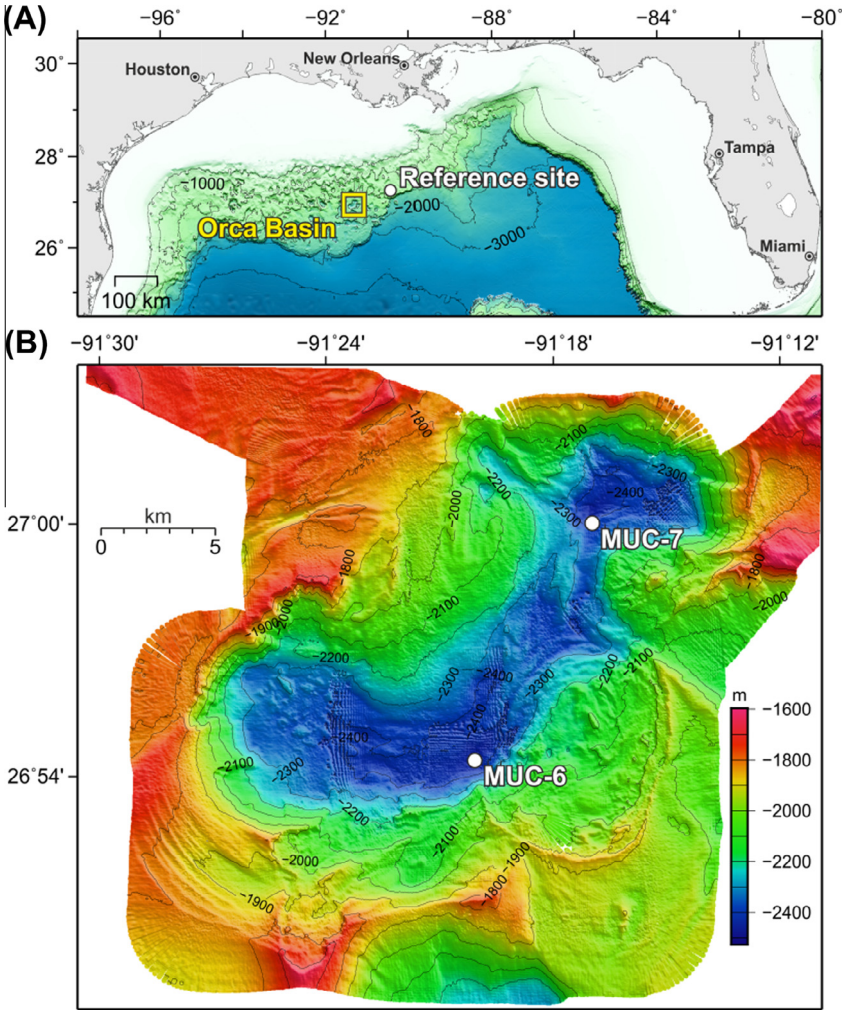

Fig. 1. Location of Orca Basin and the reference site in the northern Gulf of Mexico (A) and bathymetric map of Orca Basin (B, 20 m horizontal resolution, based on multibeam data acquired during RV *Atlantis* expedition 18-2) showing multicorer sampling locations in the southern and northern sub-basins.

stored at room temperature before analysis. For hydrogen analysis, 2 mL of sediment was transferred to helium-purged 10-mL headspace vials using a cut-off syringe and crimp-capped. The samples were stored and equilibrated for 96 h at *in situ* temperature (5 °C) before shipboard analysis. Sediment samples for intact polar lipids, trimethylamine (TMA) and DMSP in the solid phase were stored at −20 °C. Sediment samples for DNA extraction were stored at −80 °C. Pore water was extracted from sediments by centrifugation at 5000 rpm for 20 min. Pore water samples for dissolved inorganic carbon (DIC), volatile fatty acids, alcohols, DMS, TMA were stored at −20 °C. Samples for sulfate analysis were preserved by adding 50 μL of 50% HCl to 1 mL of pore water, bubbled with N_2 for three minutes, and stored at 4 °C. Samples for chloride analysis were preserved by adding 100 μL of HNO_3 to 1.5 mL of pore water. The residual sediments from pore water extraction were collected for determination of the content and stable isotopic composition of total organic carbon (TOC). Live sediments for stable isotope tracer experiments were taken from a parallel multicore sectioned into three 20 cm intervals, transferred to glass bottles, flushed with N_2 and stored at 4 °C.

2.2. Biogeochemical analyses

Salinity of pore water was determined with a handheld refractometer (Atago, Co. Ltd., Japan) after dilution. Methane concentrations were determined by injecting 1 mL headspace gas into a ThermoFinnigan TraceGC equipped with a flame ionization detector. Methane and other hydrocarbons were separated isothermally at 40 °C on a Carboxen-1006 PLOT fused-silica capillary column (0.32 mm × 30 m; Supelco, Inc., USA). Concentrations were calculated by comparison to a certified methane standard (Scott Specialty Gases®). The analytical precision determined from replicate measurement of standards was better than 1.2%. Analysis of methane-$\delta^{13}C$ values was performed on a gas chromatography combustion isotope ratio mass spectrometry (GC–C-IRMS) system combining a ThermoFinnigan Trace GC Ultra with a DELTA Plus XP mass spectrometer via a ThermoFinnigan GC Combustion III interface as described previously (Ertefai et al., 2010). Sulfide was quantified using a spectrophotometer (Cline, 1969). Chloride concentrations of diluted pore water samples were quantified using a Dionex DX5000 ion chromatograph (Joye et al., 2004, 2010). Sulfate concentrations of diluted pore water samples were measured on the same system after filtration through an OnGuard II Ag/H matrix ion resin cartridge to remove Cl^-. Headspace hydrogen concentrations were measured after 4 days of incubation at 5 °C on a Peak Performer 1 Reduced Gas Analyzer equipped with a mercury oxide detector (Peak Laboratories, USA; Hoehler et al., 1998; Lin et al., 2012). Pore water hydrogen concentrations were calculated from headspace concentrations and the solubility constant for H_2 corrected for temperature and salinity (Crozier and Yamamoto, 1974) as described by Lin et al. (2012). Dissolved inorganic carbon concentration and $\delta^{13}C$ was measured by injecting 1 mL headspace gas after acidification of pore water with 0.2 mL of 0.1 M phosphoric acid (H_3PO_4) into a gas chromatography isotope ratio mass spectrometry system consisting of a Hewlett–Packard 5890 GC equipped with a 6 m Poroplot Q column held at 35 °C and a Finnigan Mat DELTA S IRMS. Concentrations and carbon isotopic compositions of volatile fatty acids in the pore water were analyzed by using a liquid chromatography-isotope ratio mass spectrometry system, which consisted of a ThermoFinnigan Surveyor high performance liquid chromatograph (HPLC) equipped with a VA Nucleogel Sugar 810-H column (300 × 7.8 mm; Macherey–Nagel, Germany) and a guard column of the same material linked to a DELTA Plus XP IRMS via a ThermoFinnigan LC Isolink interface (Heuer et al., 2006). Methanol in pore water was determined by a custom-built purge and trap pretreatment system connected to a Hewlett–Packard GC 5890 series II with an FID and Alltech Heliflex® AT-Q capillary column (30 m × 0.32 mm I.D.; Alltech Associates, Inc., Deerfield, US) (Zhuang et al., 2014). The dissolved pool of DMS and DMSP (hereafter, $DMS(P)_d$), and dissolved TMA in the pore water were measured in one analytical step, and total base-hydrolysable DMS and DMSP (hereafter $DMS(P)_T$) as well as base-extractable TMA in the sediment were quantified simultaneously. Briefly, $DMS(P)_d$ and TMA in the pore water or base-hydrolysable $DMS(P)_T$ and TMA in the sediment were released by the addition of NaOH, pre-concentrated with a purge and trap procedure, and analyzed on a Trace GC 2000 (Thermo Finnigan, Milan, Italy) coupled to a DSQ II MS (Thermo Finnigan, Texas, USA) with a Rtx®-Volatile Amine Column (30 m × 0.32 mm I.D., Restek GmbH, Homburg, Germany; Zhuang, 2014). The detection limit for DMS and TMA was 0.1 nM and 20 nM respectively. Stable carbon isotopic ratios of sediment-extracted TMA and DMSP were analyzed using a GC–C-IRMS system combining a ThermoFinnigan Trace GC Ultra with a DELTA Plus XP mass spectrometer via a ThermoFinnigan GC Combustion III interface. In brief, ~5 g sediment was placed in a 10-mL glass vial to which 1 mL of a 5 M NaOH was added and sealed immediately with a butyl stopper. After heating at 60 °C for 10 min, 800 μL gas samples were taken from the headspace for GC–C-IRMS analysis. Determination of TOC and $\delta^{13}C_{TOC}$ were conducted on pre-weighed, freeze-dried, decarbonatized sediment (corrected for weight of precipitated salts) using a ThermoScientific Flash 2000 elemental analyzer coupled to a ThermoScientific DELTA V Plus IRMS via a ThermoScientific ConFlo IV interface.

2.3. Stable isotope tracer experiment and radiotracer microbial activity measurements

Methanogenic activity was independently assessed at the University of Bremen using stable isotope tracers and at the University of Georgia, Athens, using radioactive tracers. Sediments used in ^{13}C labeling experiments were obtained from parallel cores of multicorer casts MUC-6 (southern basin) and MUC-7 (northern basin). Samples for ^{14}C-labeling experiments were collected from a parallel core of multicorer cast MUC-7.

Table 1
Different treatments of substrates and headspace gases applied in the stable isotope tracer experiment.

	Treatment 1	Treatment 2	Treatment 3	Treatment 4	Treatment 5
Substrate	30 mM bicarbonate	30 mM bicarbonate	800 μM acetate	500 μM methanol	None
Headspace gas	80% H_2, 20% CO_2	97% N_2, 3% H_2	100% N_2	100% N_2	100% N_2

The potential of different substrates to support methanogenesis was assessed in slurry incubations with 20% ^{13}C-labeled substrates (bicarbonate, acetate, methanol; acetate was labeled on the methyl carbon). Slurries were prepared in a glove box under a reducing atmosphere (N_2:H_2, 97:3) from 1:1 sediment and anoxic artificial brine medium (major ion composition based on Schijf, 2007). Five different combinations of three labeled substrates and headspace gases (overpressure of 1.5 bar; Table 1) were amended to sediment from the southern basin (MUC-6, 0–20 cm), the northern basin (MUC-7, 0–20 cm), a non-brine reference site as a positive control, and sterilized samples from each site (autoclaved prior to substrate amendment) as a negative control.

To investigate methanogenic potential, all samples were incubated for 181 days and constantly agitated gently in a water bath in the dark. As previous studies have shown that maximum methane production rates in sediments occurred at ~30 °C (Zeikus and Winfrey, 1976; Schulz et al., 1997), the production of methane in Orca Basin could be subject to temperature limitation under *in situ* conditions (5 °C). Thus, we incubated Orca Basin sediments at 30 °C to stimulate methanogenic activity. Production of methane from the ^{13}C-labeled substrates was determined by monitoring the stable carbon isotope composition of methane in the headspace at nine time points. Samples were stored by injecting 1.5 mL headspace gas to replace a saturated NaCl solution (pH 1–2 adjusted by 1 M HCl) in a fully filled 10 mL headspace vial. The samples were placed upside down and stored at 4 °C until processing. The statistical significance of the increase of $\delta^{13}CH_4$ during incubation was assessed using one-way analysis of variance (one-way ANOVA) with the significance level (α) set at 0.1. Methane production rates were calculated from methane concentrations ($C_{methane}$), the increases of the fractions of ^{13}C in methane ($\Delta F^{13}C_{methane}$) over time (t), isotopic fractionation factor α (bicarbonate: 1.04; acetate: 1.02; methanol: 1.07; methylamine: 1.06; Krzycki et al., 1987; Summons et al., 1998; Whiticar, 1999), and the fractions of ^{13}C in the amended substrates (e.g., $F^{13}C_{methanol} = 0.2$; Eq. (1); cf. Wegener et al., 2012):

$$\text{Methane production rate} = C_{methane} \times \alpha \times \frac{\Delta F^{13C}\text{methane}}{F^{13C}\text{substrate} \times t} \quad (1)$$

The fractions of $F^{13}C$ in methane and substrates were calculated from the isotope ratios $F^{13}C = R^{13}C/^{12C}/(R^{13}C/^{12C} + 1)$, where R was the ratio of ^{13}C and ^{12}C.

Methanogenesis rate measurements were conducted through radiotracer experiments with ^{14}C-labeled substrates on sediment from the northern basin, using a method described previously (Bowles et al., 2011). Briefly, intact sediment samples were introduced into a modified Hungate tube, and injected with ^{14}C-bicarbonate (500 kBq), 2-^{14}C-acetate (250 kBq) and ^{14}C-methylamine (99 kBq). Due to the spike of the radiotracers, final pore water concentrations of 125 μmol L^{-1}, 62 μmol L^{-1} and 25 μmol L^{-1} were achieved for bicarbonate, acetate and methylamine, respectively. Hence, methanogenic activity from acetate and methylamine might have been stimulated by the addition of substrates and the methane production rates might not represent the *in situ* rates. After 120 h of incubation at 5 °C, microbial activities were terminated by injecting 2.5 mL 2 M NaOH into the samples through a syringe and needle, and headspace was created by gently pulling the plunger to the base of the Hungate tube. ^{14}C-methane was stripped from the headspace with air, purified from volatile ^{14}C-labeled non-methane components such as $^{14}CO_2$, ^{14}C-acetate and ^{14}C-methylamine via a series of traps and combusted in Ni-Ti alloy tubing filled with CuO needles at 800 °C. ^{14}C–CO_2 formed from ^{14}C-methane was trapped in ScintiSafe Gel cocktail mixed with Carbosorb E (5:1 ratio) and counted on a LS Beckman 6500 liquid scintillation counter. Methanogenesis rates from methylamine are expressed as turnover rates per day as the pore water concentrations of methylamine were not measured. Although the concentrations of methylamine were unknown, TMA concentrations were determined and previous studies suggested that this compound behaves biogeochemically similar to methylamine (e.g., distribution, production, adsorption and consumption), in particular in the context of methanogenesis (King et al., 1983; Wang and Lee, 1994, 1995). Furthermore, anaerobic oxidation of methane (AOM) and sulfate reduction rates were measured with $^{14}CH_4$ (~30 kBq) and $^{35}SO_4^{2-}$ (~150 kBq) radiotracers in the northern basin, and the details of the method and rate calculations have been described previously in Joye et al. (2010).

2.4. Intact polar and core lipid analysis

Wet sediment samples were amended with an internal standard (C_{21}-PC, Avanti Polar Lipids Inc., Alabaster, AL, USA) prior to solvent extraction using a modified Bligh & Dyer protocol (Sturt et al., 2004). The total lipid extract (TLE) was dried under a stream of N_2 and stored at −20 °C until measurement.

Intact polar and core lipids were quantified by injecting an aliquot of the TLE dissolved in methanol:dichloromethane (9:1, v:v) on a Dionex Ultimate 3000 ultra-high performance liquid chromatography (UPLC) system connected to a Bruker maXis Ultra-High Resolution quadrupole time-of-flight tandem mass spectrometer (qTOF-MS) equipped with an ESI ion source operating in positive mode (Bruker Daltonik, Bremen, Germany). The mass spectrometer was set to a resolving power of 27000 at m/z 1222 and every analysis was mass-calibrated by loop injections of a

calibration standard and correction by lock mass, leading to a mass accuracy of better than 1–3 ppm. Ion source and other MS parameters were optimized by infusion of standards into the eluent flow from the LC system via a T.

Analyte separation was achieved using reversed phase UPLC on an Acquity UPLC BEH C_{18} column (1.7 μm, 2.1 × 150 mm, Waters, Eschborn, Germany) maintained at 65 °C as described by Wörmer et al. (2013). In brief, analytes were eluted at a flow rate of 0.4 ml min^{-1} using linear gradients of methanol:water (85:15, eluent A) to methanol: isopropanol (50:50, eluent B) both with 0.04% formic acid and 0.1% NH_3. The initial condition was 100% A for 2 min, followed by a gradient to 15% B at 0.1 min and a gradient to 85% B at 18 min. The column was then flushed with 100% B for 8 min.

Lipids were identified by retention time as well as by accurate molecular mass and isotope pattern match of proposed sum formulas in full scan mode as well as MS^2 fragment spectra (for structures refer to Fig. S2). Identification of polyunsaturated archaeols by UPLC-MS^2 is described in Zhu et al. (2016). Integration of peaks was performed on extracted ion chromatograms of ±10 mDa width and included the $[M+H]^+$, $[M+NH_4]^+$, and $[M+Na]^+$ ions. Where applicable, double charged ions were included in the integration. Lipid abundances were corrected by the relative response of representative archaeal lipid standards versus the internal standard determined via an external calibration curve (Elling et al., 2014). The abundances of glycerol dibiphytanyl glycerol tetraethers (GDGTs), hydroxy GDGTs (OH-GDGTs) and glycerol dialkanol diethers (GDDs) were corrected for the response factor of purified acyclic GDGT. The abundances of archaeol (AR) and hydroxyarchaeol (OH-AR) and their unsaturated derivatives were corrected for the response of purified AR. Similarly, the abundances of intact polar lipids were corrected for the response factors of purified monoglycosidic archaeol (1G-AR), diglycosidic archaeol (for 2G-AR, phosphoinositol-AR (PI-AR), 2G-OH-AR, PI-OH-AR, and glycosyl-phosphatidylglycerol-AR (G-PG-OH-AR)), acyclic 1G-GDGT (for 1G- and 1G-OH-GDGTs), 2G-GDGT (for 2G- and 2G-OH-GDGTs) and 1G-PG-GDGT (for HPH-GDGTs).

For stable carbon isotope analysis of lipids, the selected TLEs were further separated into three fractions comprising archaeols (F1), hydroxyarchaeols (F2) and GDGTs (F3) using three-step orthogonal semi-preparative high-performance liquid chromatographic purification comprising normal phase separation of polar and apolar fractions according to Zhu et al. (2013), normal phase separation of archaeols, hydroxyarchaeols, and GDGTs using the method of Liu et al. (2012a) and a final cleanup step using reversed phase chromatography according to Zhu et al. (2013). Fractions F1 and F2 were derivatized using bis-(trimethylsilyl) trifluoroacetamide in pyridine for 1 h at 70 °C. Biphytanyl (C_{40} isoprenoid) side chains were released from GDGTs in fraction F3 using boron tribromide and subsequent reduction with lithium triethylborohydride (Bradley et al., 2009). Stable carbon isotope ratios of F1–F3 were determined in triplicate on a Thermo Finnigan Trace GC Ultra coupled to a DELTA Plus XP isotope ratio mass spectrometer via a GC Combustion Interface III. Compounds were separated on a RTX-5MS fused silica capillary column (30 m × 320 μm × 0.25 μm, Restek, Bad Homburg, Germany) using a temperature programme of 60 °C (held 1 min) to 150 °C at 15 °C min^{-1} and then to 320 °C at 4 °C min^{-1} (held 22.5 min).

2.5. Molecular analysis

DNA was extracted with the MOBIO (Carlsbad, CA) PowerSoil kit following the manufacturer's protocol. Prior to extraction, samples were centrifuged at maximum speed (16,000*g*) for 5 min and the overlying liquid was decanted. The archaeal 16S rRNA gene was amplified with Speedstar DNA polymerase (Takara) using universal primers B8f (Huber et al., 2002) and 1492r (Teske et al., 2002) and the manufacturers recommended concentration for the buffer, dNTPs and polymerase. Amplification was performed in a thermal cycler (iCycler, Biorad) under the following conditions: initial denaturation at 95 °C for 4 min, 25 cycles of 95 °C for 10 s, 52 °C for 15 s and 72 °C for 20 s, a final extension of 72 °C for 10 min. PCR products were electrophoresed on a 1% agarose gel and visualized with ultraviolet light after staining with GelRed (Biotium). PCR products were purified with the Qiagen PCR purification kit. Clone libraries were constructed from PCR products with the TOPO TA Cloning Kit and TOP10 chemically competent cells (Invitrogen, Carlsbad, CA) according to the manufacturer's instructions. Individual white colonies were arbitrarily picked and sent to Genewiz (South Plainfield, NJ) for Sanger sequencing using vector primers M13F and M13R. DNA alignments and sequence-associated taxonomic assignments were determined using the SILVA 111 small subunit rRNA database (Pruesse et al., 2012; Quast et al., 2012) and the ARB phylogenetic and sequence analysis program (Ludwig et al., 2004).

2.6. Thermodynamic calculations

The Gibbs energy per mole of reaction under *in situ* conditions was calculated for different metabolic pathways (Table S1). Standard-state energy yields (ΔG^0) were calculated and corrected for temperature with Gibbs functions, $\Delta G^0 = \Delta H^0 - T\Delta S^0$ (Stumm and Morgan, 1981), using thermodynamic data of products and reactants for dissolved aqueous species from Wagman et al. (1982). The activity of SO_4^{2-}, HCO_3^-, HS^-, and NH_4^+ was computed through the input of major ions (Ca^{2+}, Mg^{2+}, Na^+, K^+, Cl^-, dissolved inorganic carbon, SO_4^{2-}, NH_4^+ and HS^-) (Schijf, 2007) at *in situ* pH and temperature with Visual MINTEQ version 3.0, using the specific ion interaction theory activity coefficient model; activity coefficients of dissolved gases were set to 1.

3. RESULTS

3.1. Geochemistry of Orca Basin sediments

Pore water salinities varied slightly between 261‰ and 273‰ in the southern basin (Fig. 2A) and decreased with

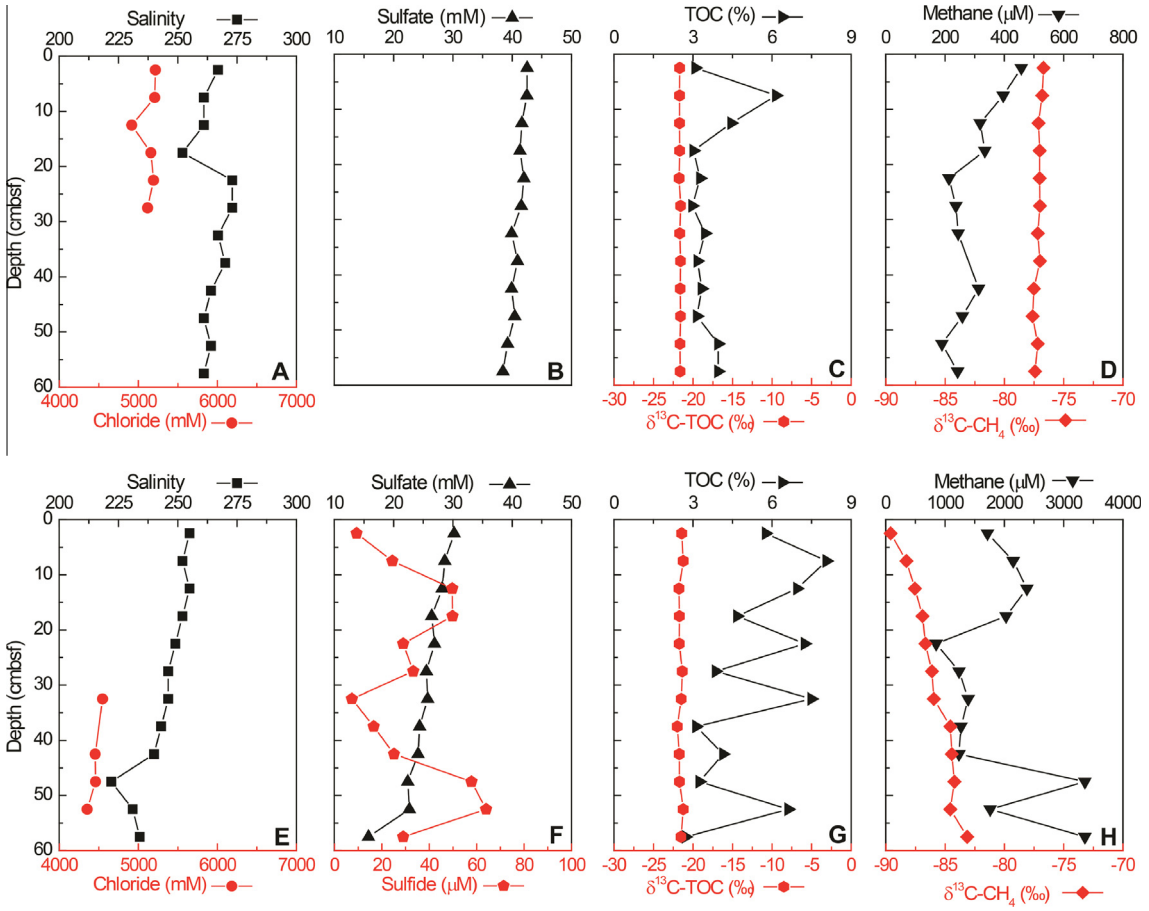

Fig. 2. Depth profiles of geochemical parameters (A, E) salinity and chloride, (B, F) sulfate and sulfide, (C, G) TOC and δ^{13}C-TOC, (D, H) methane and $\delta^{13}C$–CH_4 in pore water and sediments from southern (A–D) and northern (E–H) Orca Basin.

depth from 255‰ to 222‰ in the northern basin (Fig. 2E). The average concentration of chloride in the pore waters from the southern basin was 5134 mM (Fig. 2A), about nine times of that at the reference site (550 mM, Fig. S1A). In the northern basin, chloride concentrations were slightly lower, with an average value of 4453 mM between 32.5 and 52.5 cm (Fig. 2E). Pore water sulfate concentrations varied between 38 and 43 mM in the southern basin (Fig. 2B). In contrast, sulfate declined with sediment depth from 30 mM to 16 mM in the northern basin concurrent with the appearance of low amounts of sulfide (Fig. 2F). The TOC content of the sediment in the southern (average of 3.7%, Fig. 2C) and northern basin (average of 5.3%; Fig. 2G) was much higher than at the reference site (average of 0.6%, Fig. S1C). TOC in the southern basin sediment was constant at ~3% except for a peak at 7.5 cm (~6%), while the values were highly variable between ~3% and ~8% with an overall decreasing trend with depth in the northern basin. The average δ^{13}C value of TOC was −21‰ in the southern basin and −22‰ in the northern basin. Methane accumulated in the upper 25 cm of the southern basin sediments (~460 μM) and decreased downcore to 200–250 μM (Fig. 2D). Methane was depleted in ^{13}C within a narrow range of −76‰ to −77‰ throughout the core (Fig. 2D). In the northern basin, methane was more abundant and fluctuated between 850 and 3360 μM (Fig. 2H). The δ^{13}C value of methane was −90‰ at 2.5 cm, increased with increasing depth, and reached a maximum of −83‰ near the base of the core (57.5 cm; Fig. 2H). In contrast to the brine basin, methane concentrations were very low in the sulfate-bearing sediment at the reference site (mostly <1 μM; Fig. S1B).

3.2. Potential methanogenic substrates and thermodynamics

Hydrogen concentrations were uniformly low in the sediment of the southern and northern basins (~0.25 nM; Fig. 3A, G). DIC concentrations were generally less than 10 mM with δ^{13}C values of ~−20‰ (Fig. 3B, H). Thermodynamic calculation showed that hydrogenotrophic methanogenesis under *in situ* conditions were mostly endergonic in the southern and northern Orca Basins (southern basin: ΔG: −1 to 20 kJ mol^{-1}, Fig. 4A; northern basin: ΔG: 10–14 kJ mol^{-1}, Fig. 4C). Acetate and other volatile fatty acids were below the detection limit (5 μM; Heuer et al., 2006) in both the southern and northern basins. Assuming acetate concentrations of 5 μM (limit of detection), the maximum energy yield of acetoclastic methanogenesis was between −14 and −22 kJ mol^{-1} (Fig. 4A, C).

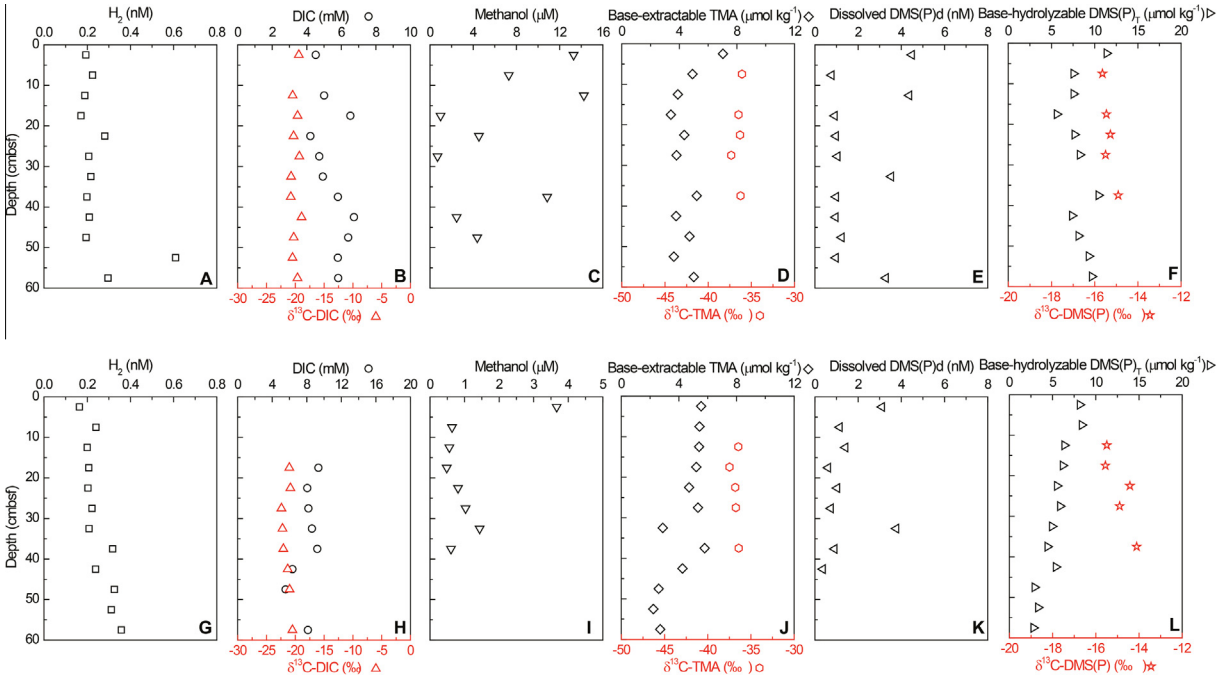

Fig. 3. Depth profiles of potential methanogenic substrates (A, G) hydrogen, (B, H) DIC and δ^{13}C-DIC, (C, I) methanol, (D, J) base-extractable TMA and δ^{13}C-TMA, (E, K) dissolved DMS(P)$_d$, (F, L) base-hydrolysable DMS(P)$_T$ and δ^{13}C-DMS(P) in pore water and sediments from the southern (A–F) and northern (G–L) Orca Basin.

Methanol was relatively abundant in the southern basin and the concentrations varied considerably between 0.7 μM and 14 μM (Fig. 3C). In the northern basin, methanol concentrations were lower (~1 μM), with an exception of 3.7 μM at the sediment surface (2.5 cm) (Fig. 3I). Thermodynamically, methanogenesis from methanol was highly exergonic in the southern and northern basins (ΔG: −182 to −229 kJ mol^{-1}, Fig. 4B, D).

Dissolved TMA was only detectable in the pore water at 2.5 cm (southern basin: 48 nM; northern basin: 41 nM; detection limit: 20 nM), whereas the total base-extractable TMA in the sediment was much more abundant in both the southern (3.4–7.0 μmol kg^{-1}, Fig. 3D) and northern basins (2.2–5.5 μmol kg^{-1}, Fig. 3J). At the reference site, TMA concentrations in the sediment were generally lower by a factor of three (0.8–2.3 μmol kg^{-1}, Fig. S1D). The pore water concentrations of the dissolved pool of DMS and DMSP (DMS(P)$_d$) in the southern basin were variable between 0.8 nM and 4.5 nM (Fig. 3E). In the northern basin, DMS(P)$_d$ concentrations slightly decreased with depth, with an exception of a maximum at 32.5 cm (3.8 nM; Fig. 3K). The total base-hydrolyzable DMSP (DMS(P)$_T$) including DMS, dissolved and particulate DMSP were three orders of magnitude higher than those of DMS(P)$_d$ in the pore water of the southern and northern basins, with an average of 8.5 and 5.4 μmol kg^{-1}, respectively (Fig. 3F, L). Likewise, the energy yield was much higher for methanogenesis from TMA and DMS under *in situ* conditions (Fig. 4B, D). The δ^{13}C value of base-extractable TMA in the sediment was on average −37‰ in the southern and northern basins (Fig. 3D, J). The δ^{13}C signature of DMS evolved from base-hydrolysis of DMSP was between −16‰ and −14‰ (Fig. 3F, L) and became progressively depleted with depth.

3.3. Stable isotope and radioactive tracers experiments

Stable isotope tracer experiments with ^{13}C-bicarbonate and H_2, ^{13}C-acetate, and ^{13}C-methanol were conducted to trace the utilization of different substrates for methanogenesis in Orca Basin sediments. In the sediments from the reference site, methane was below detection for all types of substrates at every time point. In sediment from the southern basin, $\delta^{13}CH_4$ did not change significantly over time for all types of substrates added (Table S2). Likewise, samples from the northern basin amended with ^{13}C-bicarbonate and H_2 as well as ^{13}C-acetate did not show significant increase of $\delta^{13}CH_4$ after 181 days of incubation (Fig. 5; Table S3). A significant increase of $\delta^{13}CH_4$ over time was observed in samples amended with ^{13}C-methanol ($\alpha = 0.1$, $p = 0.08$). $\delta^{13}CH_4$ in the duplicate incubations increased progressively from −87‰ at day 3 to −56‰ and −87‰ to −67‰ at day 112, respectively and did not increase further (Fig. 5; Table S3). The killed controls and negative controls (no substrate plus N_2 headspace) did not show significant changes in $\delta^{13}CH_4$ over time (Tables S2 and S3).

Radiotracer experiments showed that methanogenesis from ^{14}C-labeled methylamine was detected in the shallow sediment of the northern basin. The turnover rates of

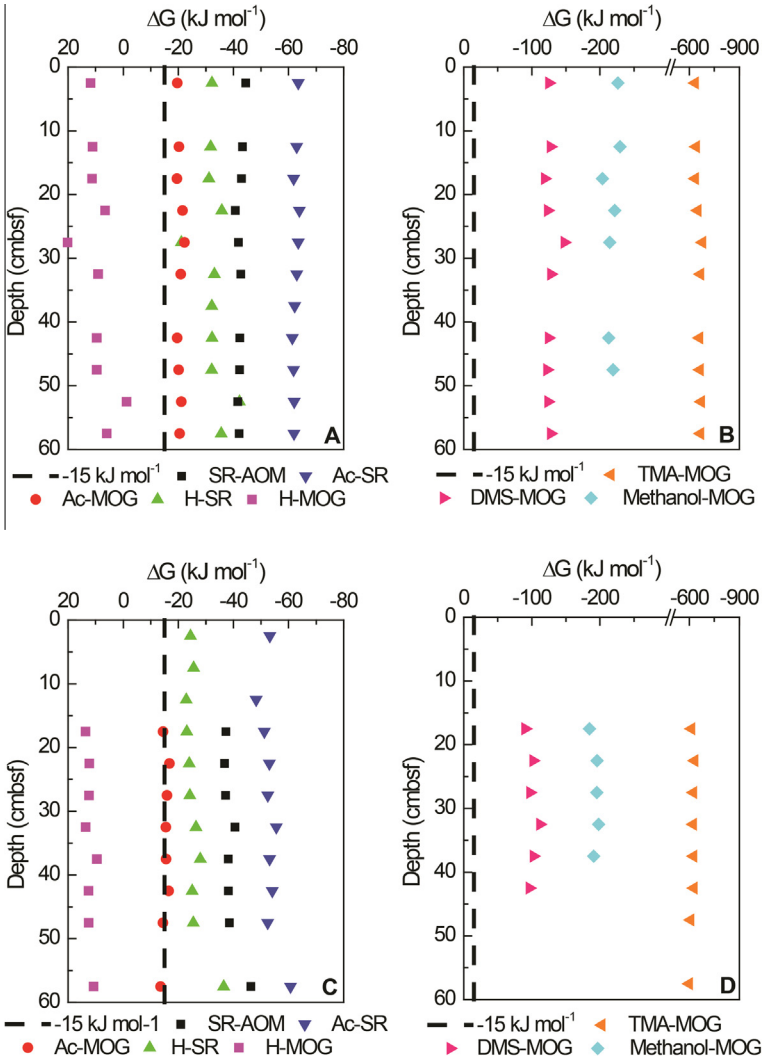

Fig. 4. Depth profiles of Gibbs energy (ΔG) yield in the southern (A and B) and northern (C and D) Orca Basin. H-MOG: hydrogen-based methanogenesis; Ac-MOG: acetate-based methanogenesis, we used the detection limit of 5 μM for acetate concentrations; AOM-SR: sulfate reduction coupled AOM; TMA-MOG: TMA-based methanogenesis, we used 20 nM where TMA concentrations were below the detection limit; DMS-MOG: DMS-based methanogenesis; Methanol-MOG: methanol-based methanogenesis; H-SR: hydrogen-based sulfate reduction, sulfide was assumed as 10 μM; Ac-SR: acetate-based sulfate reduction. The dashed line indicates the minimum biological energy quantum for life sustainment (-15 kJ mol^{-1}). ΔG was not calculated at some depths due to the incomplete coverage of geochemistry data.

methylamine were 1.2×10^{-6} and 2.1×10^{-6} per day at 2.5 cm and 7.5 cm, respectively. In contrast, no conversion to methane from ^{14}C-labeled bicarbonate and acetate was observed. In the northern basin, AOM rates were below detection (<1 pmol cm^{-3} d^{-1}) while sulfate reduction rates were relatively high (10–30 nmol cm^{-3} d^{-1}).

3.4. Archaeal 16S ribosomal RNA genes analysis

Sanger sequencing targeting the archaeal 16S rRNA gene revealed diverse archaeal populations in Orca Basin sediments. Sequences related to the Marine Group I (MG-I) *Thaumarchaeota* dominated the clone library sequence assemblages in the surface sediment (0–5 cm, 28 archaeal sequences, 61% MG-I) and at 55–60 cm (37 archaeal sequences, 73% MG-I) of the southern basin (Fig. 6). Other sequences were related to the Marine Group II *Euryarchaeota* and the euryarchaeal genus *Methanohalophilus*. In the deep sediment sample (55–60 cm) from the southern basin, sequences related to the Marine Group III, the Deep-Sea Hydrothermal Vent Euryarchaeotal Group 5 (DHVE-5) and ANME-1a, ANME-1b and ANME-2c clades were detected (Fig. 6). Compared to the southern basin, archaeal sequences were more diverse in the surface sediment of the northern basin (0–5 cm, 56 archaeal sequences), indicated by the occurrence of sequences related to the ANME-2a and the Miscellaneous Crenarchaeotic Group (MCG). In contrast, much lower diversity was observed in the deep sediment of the northern basin (50–55 cm, 33 archaeal sequences), in which

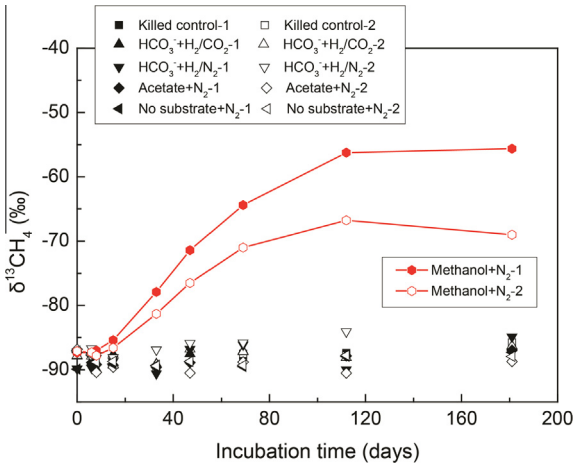

Fig. 5. Time series of $\delta^{13}C$–CH_4 in duplicate sediment samples amended with either ^{13}C-labeled bicarbonate, acetate or methanol as well as killed control samples from northern Orca Basin.

Methanohalophilus accounted for 85% of the sequences, the rest being related to MG-I.

3.5. Intact polar and core lipid analysis

The relative abundances of major core and intact polar lipid groups were highly similar across the sampled sediment intervals as well as between the southern and northern basin sites (Fig. 7). Archaeal tetraether lipids (GDGTs) and derivatives such as hydroxylated GDGTs and GDDs with zero to five cycloalkylations were the major components of the core lipid pool. The diether lipids archaeol and hydroxyarchaeol as well as their unsaturated homologues containing up to seven double bonds comprised 22–43% of the core lipids. Intact polar lipids accounted for 3–7% of total archaeal lipids with an exception of 14% at 50–55 cm sediment depth in the northern basin (Tables S4 and S5). Among the intact polar lipids, intact polar glycosidic and phospho-glycosidic GDGTs and hydroxy GDGTs dominated the intact polar lipid pool in most samples (Fig. 7; Tables S4 and S5). Intact polar diether lipids consisted of saturated archaeols and hydroxyarchaeols with glycosidic and phosphatidic headgroups.

The $\delta^{13}C$ values of GDGT-derived biphytanes were between −17‰ and −21‰ (Fig. 8; Table S6). In contrast, $\delta^{13}C$ values of *sn*-2-hydroxyarchaeol were highly negative at −77‰ to −78‰ in all samples (Fig. 8; Table S6). Monounsaturated *sn*-2-hydroxyarchaeol as well as the *sn*-3 isomer of hydroxyarchaeol were only detected in the 50–55 cm sample from the northern basin and showed similar ^{13}C depletion as *sn*-2-hydroxyarchaeol. Archaeol was less depleted in ^{13}C than hydroxyarchaeol derivatives in all samples except the one at 50–55 cm sample in the northern basin (−78‰; Table S6). Monounsaturated archaeol, for which an isotope value could only be determined in this sample, was less depleted (−59‰) than archaeol (−78‰; Table S6).

4. DISCUSSION

4.1. Geochemistry

Pore water salinity reached up to 273‰ in the Orca Basin, and such high salinities limit the active microbial community to extremely halophilic bacteria and archaea that are able to thrive at salinities over 180‰ (Oren, 2008). Despite the low amount of sulfide, the decrease of sulfate potentially indicated the occurrence of sulfate reduction. In Orca Basin, sulfide production from sulfate

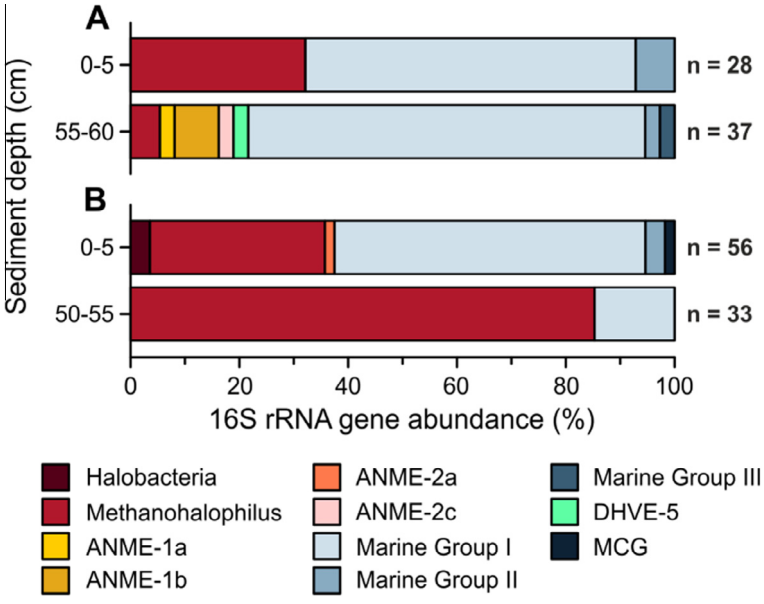

Fig. 6. Relative abundances of archaeal 16S rRNA gene sequences at 0–5 cm and 50–55/55–60 cm sediment depth in southern (A) and northern (B) Orca Basin.

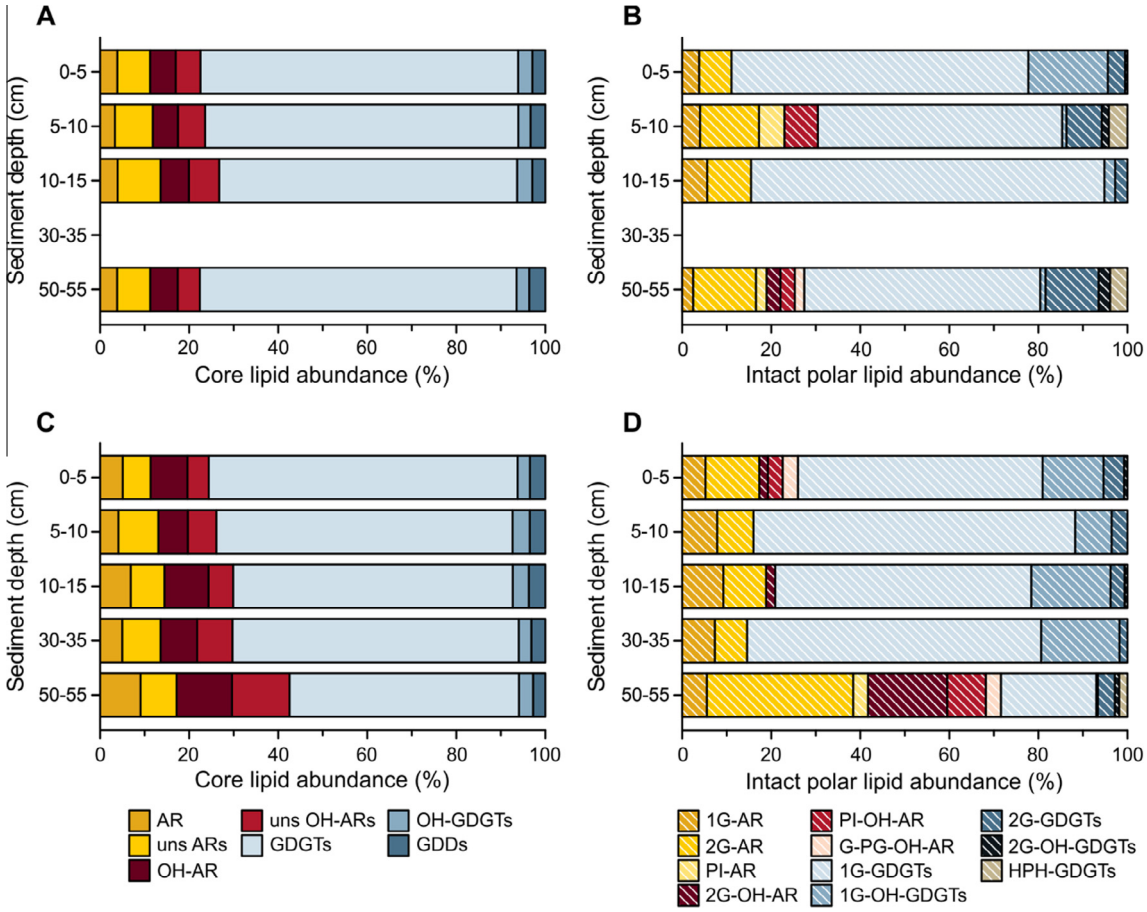

Fig. 7. Relative abundances of archaeal core and intact polar lipids in sediment from the southern (A, B) and northern (C, D) Orca Basin. Core lipid nomenclature: AR: archaeol; uns ARs: summed unsaturated archaeols (1–7 double bonds); OH-AR: hydroxyarchaeol; uns OH-ARs: summed unsaturated hydroxyarchaeols (1–7 double bonds); GDGTs: glycerol dibiphytanyl glycerol tetraethers; OH-GDGTs: hydroxy GDGTs; GDDs: glycerol dialkanol diethers. Intact polar lipid nomenclature indicates headgroup and core lipids combinations: 1G: monoglyosyl; 2G: diglycosyl; PI: phosphoinositol; G-PG: glycosyl-phosphatidylglycerol; HPH: hexose-phosphohexose. Lipid structures are shown in Fig. S2.

reduction might be masked by precipitation of sulfide given the abundant reduced iron and metastable iron sulfides found in these sediments (Wiesenburg et al., 1985). In contrast to the reference site, the high TOC contents and the $\delta^{13}C$ values likely reflect a combination of planktonic organic matter input with some admixtures of terrigenous organic matter and enhanced preservation in the hypersaline brine (Northam et al., 1981; Kennicutt et al., 1992).

Despite the presence of sulfate, considerable methane concentrations were observed in the sediment. In deep-sea brine pools, methane was assumed to originate from biogenic (e.g., Mediterranean Sea; Charlou et al., 2003), thermogenic (e.g., Red Sea; Faber et al., 1998), or mixed biogenic and thermogenic sources (e.g., Gulf of Mexico; Joye et al., 2005). The strongly depleted $\delta^{13}C$ values of methane in Orca Basin (−77‰ to −89‰), are indicative of microbial methanogenesis. As methanogenesis from hydrogen and acetate is likely to be inhibited due to competition for these substrates with sulfate reducers, the coexistence of substantial amounts of biological methane with sulfate at both brine sites might result from methanogenesis from non-competitive substrates. Under the assumption that substrate limitation leads to ^{13}C-enriched methane (Kelley et al., 2012), the ^{13}C-depletion of methane may also reflect the availability of substrates for methanogenesis.

4.2. Methanogenic substrates, thermodynamic feasibility and carbon isotope relationships

The highly negative $\delta^{13}C$ values of methane (−77‰ to −89‰) in Orca Basin are within the range expected for hydrogenotrophic methanogenesis (cf. Whiticar et al., 1986). However, hydrogen concentrations in the Orca Basin were three orders of magnitude lower than values reported for shallow seafloor brine pools in the Gulf of Mexico (Joye et al., 2009). In marine sediments, low H_2 concentrations are sustained by close coupling of microbial H_2 production and consumption via interspecies hydrogen transfer in syntrophic relationships (Hoehler et al., 1998; Lin et al., 2012). In this way, sulfate reducing bacteria are able to sustain H_2

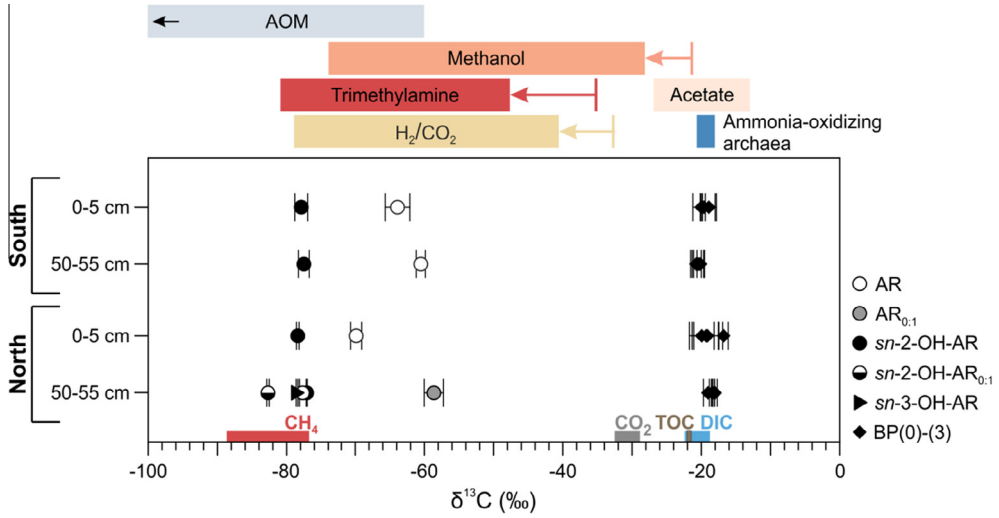

Fig. 8. Stable carbon isotopic composition ($\delta^{13}C$ vs. the Vienna Pee Dee Belemnite standard) of archaeal membrane lipids in Orca Basin sediments showing highly depleted $\delta^{13}C$ signatures of diether lipids versus relatively more enriched signatures of tetraether lipids. Arrows and colored bars above plot indicate $\delta^{13}C$ values of different methanogenic substrates and the predicted range of resulting lipid $\delta^{13}C$ values based on substrate-to-lipid fractionation in *Methanosarcina barkeri* (Londry et al., 2008; Table S3). Additionally, the range of lipid $\delta^{13}C$ values typically associated with anaerobic oxidation of methane (AOM) and ammonia-oxidizing archaea, as well as the range of $\delta^{13}C$ values of methane, TOC, DIC, and CO_2 in Orca Basin sediments are indicated. TOC $\delta^{13}C$ values were assumed for acetate and methanol. The $\delta^{13}C$ of CO_2 was calculated from $\delta^{13}C$ of DIC using ε_{CO_2-DIC} at 5 °C of −10.2 (Mook et al., 1974). Lipid nomenclature: AR: archaeol; $AR_{0:1}$: monounsaturated archaeol; *sn*-2-OH-AR: *sn*-2-hydroxarchaeol; *sn*-2-OH-$AR_{0:1}$: monounsaturated *sn*-2-hydroxyarchaeol; *sn*-3-OH-AR: *sn*-3-hydroxarchaeol; BP(0)-(3): GDGT-derived biphytanyl side chains containing zero to three cyclizations; (BP(3): crenarchaeol-derived). (For interpretation of the references to color in this figure legend, the reader is referred to the web version of this article.)

concentrations below the thermodynamic threshold required for hydrogenotrophic methanogenesis to occur. Owing to the low hydrogen concentrations, the energy yields of hydrogenotrophic methanogenesis could not meet the presumed biological energy quantum for life sustainment (−15 kJ mol^{-1}, Hoehler, 2004; Schink and Stams, 2006) in sediments from southern and northern Orca Basin. Similarly, hydrogenotrophic methanogenesis was also not detected in hydrogen-replete brine pools in the Gulf of Mexico (Joye et al., 2009), indicating that hydrogenotrophic methanogenesis might be limited by factors other than hydrogen concentrations or might generally be suppressed in hypersaline habitats (as previously suggested by Oren, 1999).

Contrary to previous studies that demonstrated high concentrations of acetate and associated methanogenesis in brines and underlying sediments in the Gulf of Mexico and the Mediterranean Sea (Joye et al., 2009; Lazar et al., 2011), the low concentrations of acetate suggest that acetoclastic methanogenesis is unimportant in Orca Basin sediments. Thermodynamic calculations also indicate the inhibition of acetoclastic methanogenesis, as sulfate reduction with acetate was energetically more favorable in the southern and northern basins (Fig. 4). Previous studies reported that limited sulfate reduction and AOM could occur in Orca Basin (Sackett et al., 1979; Wiesenburg et al., 1985). In the southern and northern basins, sulfate-dependent AOM was energetically favorable (southern basin: ΔG: −41 to −45 kJ mol^{-1}, Fig. 4A; northern basin: ΔG: −37 to −46 kJ mol^{-1}, Fig. 4C), while these energy yields need to be shared between sulfate reducing bacteria and ANME. However, rate measurements in the northern basin showed that sulfate reduction rates were between 10 and 30 nmol cm^{-3} d^{-1}, whereas AOM was not detectable. The lack of AOM could be attributable to the inhibition of AOM activity under extremely hypersaline conditions, consistent with previous studies that demonstrated a decrease of AOM rates with increasing salinity (Nauhaus et al., 2005; Avrahamov et al., 2014). The much higher rates of sulfate reduction relative to AOM indicated that sulfate reduction was not primarily coupled to AOM in Orca Basin. Instead, sulfate reducing bacteria might utilize acetate or H_2 and out-compete methanogens for these energy sources.

Furthermore, the highly depleted $\delta^{13}C$ value of methane also might rule out acetoclastic methanogenesis as the major source of methane in Orca Basin. Carbon isotopic fractionation during acetoclastic methanogenesis ranges from −35‰ to −7‰ in pure cultures (Krzycki et al., 1987; Valentine et al., 2004; Penning et al., 2006). Fermentation of organic matter would likely yield acetate with a $\delta^{13}C$ close to that of TOC (∼−22‰) and could therefore not explain the strong ^{13}C-depletion of methane. Alternatively, acetate may be derived from homoacetogenesis utilizing H_2 and CO_2 ($\delta^{13}C$-DIC ∼−20‰), which results in strong carbon isotope fractionation in the range of −50‰ to −60‰ (Gelwicks et al., 1989). Therefore, methanogenesis from acetate derived from homoacetogenesis could theoretically yield $\delta^{13}C$ signatures similar to those observed in Orca Basin sediments. At the low hydrogen concentrations in Orca Basin, however, both sulfate reducers and methanogens would likely out-compete homoacetogens (Lin et al., 2012), rendering a scenario of methanogenesis from ^{13}C-depleted acetate unlikely.

As hydrogen and acetate are unlikely substrates for methanogenesis, methane could be produced from methylated substrates in Orca Basin. Methanol was present in the southern and northern basins, implying an *in situ* imbalance of production and consumption. Known sources of methanol include fermentation of lignin and pectin, for example by bacteria such as *Haloanaerobium praevalens* which were found to be involved in pectinolytic activity in hypersaline environments (Ollivier et al., 1994). The utilization of methanol by methanogens has been documented in a range of hypersaline sediments, e.g., Big Soda Lake (Oremland et al., 1982a), Mono Lake (Oremland et al., 1993), Soap Lake (Oremland and Miller, 1993), the Dead Sea (Marvin-DiPasquale et al., 1999), and Searles Lake (Kulp et al., 2007). Thermodynamically, methanogenesis from methanol was highly favorable in the southern and northern basins (Fig. 4). Thus, methanol-dependent methanogenesis seems feasible for Orca Basin sediments and this hypothesis is further supported by incubation experiments (Section 4.3).

Both TMA and DMSP concentrations in the Orca Basin were much higher than the reference site. In hypersaline environments, abundant TMA might be derived from the breakdown of compounds such as glycine betaine that are biosynthesized as compatible solutes by halophilic microorganisms (Oren, 1990). Zhilina and Zavarzin (1990) isolated a halophilic homoacetogen from cyanobacterial mats of Sivash (Crimea) that produced methylamines and acetate from glycine betaine. Although TMA has been proposed as a central intermediate for methanogenesis in hypersaline environments owing to the ubiquity of precursor compounds (McGenity, 2010), this assumption lacks direct evidence from *in situ* abundance measurements, especially in deep-sea hypersaline sediments. The observation of elevated TMA concentrations in Orca Basin sediments highlights the importance of this low molecular weight metabolite in hypersaline environments. Analogous to TMA precursors, DMSP acts as an osmolyte in a wide variety of marine phytoplankton (Keller et al., 1989; Zhuang et al., 2011). Sedimentary DMSP might be derived from phytoplankton biomass exported from the overlying water column, which was reflected by an overall decrease in abundance with depth. It has been demonstrated that DMSP and its decomposition products such as DMS and methanethiol could significantly stimulate methane production in a variety of anoxic environments including hypersaline sediments (Kiene et al., 1986; van der Maarel and Hansen, 1997).

Likewise, methanogenesis from TMA and DMS under *in situ* conditions were highly exergonic processes in the southern and northern basins (Fig. 4). The high energy gains could support the survival of extremely halophilic methanogens, as halophiles need to divert energy for the maintenance of their osmotic equilibrium via the biosynthesis or uptake of organic compatible solutes and active ion pumping. A substrate-dependence of the upper salinity limit of methanogens has been observed in pure cultures, where methylamines facilitated growth to higher salinities (salinity: 270) than hydrogen and carbon dioxide (salinity: 120) as well as acetate (salinity: 40) (Oren, 1999). Although sulfate reduction coupled with the metabolism of methylated substrates could provide more energy than methylotrophic methanogenesis (Fig. 4), it has been demonstrated that sulfate-reducing bacteria generally do not use these non-competitive substrates (Oremland and Polcin, 1982). Collectively, abundant precursor molecules and high methanogenic energy yield would facilitate methane production from methylated substrates in Orca Basin.

Further evidence for methylotrophic methanogenesis could be inferred from $\delta^{13}C$ systematics of methane and potential precursors. Based on pure culture studies, utilization of TMA should yield methane $\delta^{13}C$ values in the range of 39–71‰ more depleted than the substrates (Summons et al., 1998; Whiticar, 1999; Londry et al., 2008). With the average $\delta^{13}C$ value of base-extractable TMA (−37‰) in the southern and northern basin, $\delta^{13}C$ values of TMA-derived methane should range between −76‰ and −108‰. The progressive depletion of $\delta^{13}C$ in DMS (i.e., evolved from base-hydrolysis of DMSP) with depth, also indicated preferential utilization of ^{12}C during microbial degradation of DMSP. Assuming a fractionation factor of 44–54‰, $\delta^{13}C$ values of DMS-derived methane should range between −58‰ and −70‰ (Oremland et al., 1989; Whiticar, 1999). Methanogenesis from methanol would yield methane with $\delta^{13}C$ values of −84‰ to −104‰ assuming $\delta^{13}C$ of TOC (−21‰) as a proxy for $\delta^{13}C$ of methanol (Krzycki et al., 1987; Oremland et al., 1989; Whiticar, 1999; Londry et al., 2008). In sum, the $\delta^{13}C$ values of methane of −77 ‰ to −89 ‰ are in the expected range for methylotrophic methanogenesis utilizing predominantly TMA and methanol and to a lesser extent DMS and DMSP. Therefore, methanogenesis in Orca Basin is likely fueled to a substantial degree by non-competitive methylated substrates.

4.3. Methanogenic activity

In the northern basin, the incorporation of ^{13}C exclusively from methanol into methane suggested that methylotrophic methanogenesis was the only quantitatively important methanogenic pathway operating in the hypersaline sediment. Based on mass balance calculations, the methane production rates were 2.7×10^{-4} and 4.4×10^{-4} nmol L^{-1} d^{-1} at day 112 for duplicate incubations, although the measured methane production rates might not represent the actual *in situ* rates as the incubation conditions were not identical to conditions in the original sediment. Similarly, ^{13}C-enriched methane was only produced from ^{13}C-labeled methylamines and methanol but not from labeled acetate and bicarbonate in hypersaline ponds in Baja California Sur, Mexico, and northern California, USA (Kelley et al., 2012). Methanogenic activities in the southern basin could be too low to be captured by the stable isotope tracer experiment or could be confined to deeper sediment layers. In contrast to the northern basin, the relatively higher salinity in the southern basin might further reduce the activity of methanogens. Furthermore, 16S rRNA sequences related to methylotrophic methanogens were less abundant in the southern basin (see Section 4.4), which may lead to lower methanogenic activity.

Radiotracer experiments using ^{14}C-labeled bicarbonate, acetate and methylamine support the significance of methylotrophic methanogenesis. Methanogenesis from ^{14}C-labeled methylamine was observed in the shallow sediment of the northern basin. No $^{14}CH_4$ methane was detected from ^{14}C-labeled bicarbonate and acetate, again suggesting the lack of hydrogenotrophic and acetoclastic methanogenesis in Orca Basin sediments. Lazar et al. (2011) demonstrated that methylotrophic methanogenesis was the only significant methanogenic pathway in shallow hypersaline sediments (0–40 cm) in the center of the Napoli mud volcano in the Eastern Mediterranean Sea. However, methylamine turnover rates in Orca Basin were by two orders of magnitude lower than in the Napoli mud volcano (Lazar et al., 2011), which may be attributed to the lower salinity in the Napoli mud volcano (<3 M Cl^-) compared to Orca Basin (~5 M Cl^-). Despite the relatively low methanogenic activity, both the stable and radioisotope tracer experiments supported a dominance of methylotrophic methanogenesis in the hypersaline sediments of Orca Basin.

4.4. Diversity of archaeal 16S ribosomal RNA genes

A large number of MG-I *Thaumarchaeota* sequences were detected in the surface sediment of southern Basin, indicating potential adaptation of Marine Group I to the hypersaline environment (Kamanda et al., 2015) or the preservation of water column-derived DNA, which has been demonstrated to occur over geologic timescales in anoxic sediments (Corinaldesi et al., 2011) and may be further enhanced by the pickling effect of highly saline fluids. Conspicuously, the euryarchaeal genus *Methanohalophilus* was also found in the southern basin. Archaea of the genus *Methanohalophilus* are obligate halophilic methanogens that have been previously detected in a wide range of hypersaline environments (Oremland et al., 1982b; Orphan et al., 2008). Cultured members of this genus are obligate methylotrophs that could grow at salinities of up to 250‰ and metabolize a variety of C_1 compounds including methylamines, methanol and methylsulfides, rather than H_2, formate, or acetate (Paterek and Smith, 1988; Liu et al., 1990). Despite the detection of putative anaerobic methane oxidizers (e.g., ANME-1a, ANME-1b and ANME-2c clades) in the deep sediment sample (55–60 cm) from the southern basin, the presence and inferred activity of AOM communities is not evident in the $\delta^{13}CH_4$ profile and the thermodynamic feasibility of AOM (ΔG ~−40 kJ mol^{-1}) is low.

Compared to the southern basin, the relative sequence abundance of *Methanohalophilus* was higher in the northern basin. In the deeper sediment, *Methanohalophilus* sequences accounted for 85% of the archaeal sequences. The elevated abundance of *Methanohalophilus*-related sequences in the northern basin clone library reflected the higher potential for methylotrophic methanogenesis compared to the southern basin inferred from substrate concentrations and labeling experiments. Collectively, 16S rRNA gene analysis provided phylogenetic evidence for the existence of a methylotrophic methanogen community in the hypersaline sediment of Orca Basin and supported the observation of higher methanogenic activity in the northern basin.

4.5. Lipid biomarkers

GDGTs and their derivatives dominated the core lipid pool in the southern and northern basins. These compounds are sourced mainly by aerobic planktonic *Thaumarchaeota* and ubiquitously found in the marine water column and sediments (Schouten et al., 2000; Wakeham et al., 2007; Liu et al., 2012a,b) and might therefore reflective of the high preservation of planktonic debris into Orca Basin (Tribovillard et al., 2008, 2009). In contrast to GDGTs, high abundances of archaeol and hydroxyarchaeol are typically not observed in marine water column and sediment samples (cf. Turich et al., 2007; Turich and Freeman, 2011). While archaeol can be found in cultured representatives of all archaeal clades (Koga and Morii, 2005; Schouten et al., 2008), high abundances of archaeol and specifically hydroxyarchaeol in marine sediments are often related to the occurrence of methanogenic and methanotrophic archaea (Sprott et al., 1990; Hinrichs et al., 1999; Rossel et al., 2011). Similarly, cellular membranes of extremely halophilic archaea consist primarily of archaeol but are devoid of hydroxyarchaeol (Kates, 1993; Koga and Morii, 2005). As the relative abundances of archaeol and hydroxyarchaeol as well as unsaturated hydroxyarchaeols are strongly correlated (Fig. 9), a common methanogenic or methanotrophic archaeal source of these lipids appears plausible.

Polyunsaturated archaeols have been reported from oxic and anoxic seawater (Zhu et al., 2016) as well as from several cultivated *Thermoplasmatales* (Golyshina et al., 2016) and extremely halophilic *Halobacteriales* strains (Nichols and Franzmann, 1992; Qiu et al., 1998; Gibson et al., 2005) and appear to be involved in adaptation of the lipid membrane to high salinities (Dawson et al., 2012). Similarly, polyunsaturated archaeols and hydroxyarchaeols are also synthesized by the methylotrophic methanogen *Methanococcoides burtonii* in response to cold temperatures (Franzmann et al., 1992; Nichols et al., 2004), but polyunsaturated hydroxyarchaeols have not been reported from environmental samples. In Orca Basin sediments, the relative abundance of unsaturated archaeols was not correlated with either archaeol or saturated and unsaturated hydroxyarchaeols, suggesting distinct sources of these lipids (Fig. 9). Therefore, unsaturated archaeols may originate predominantly from *Halobacteriales*-like archaea while unsaturated hydroxarchaeols along with saturated archaeol and hydroxyarchaeol could be synthesized by methanogenic or methanotrophic archaea.

Intact polar lipids generally accounted for 3–7% of total archaeal lipids (for structures refer to Fig. S2), which was within the range reported for marine sediments (Lipp and Hinrichs, 2009; Liu et al., 2011). The highest abundance of intact polar lipids (14%) was observed in the 50–55 cm sample from the northern basin. In most samples, intact polar glycosidic and phospho-glycosidic GDGTs and hydroxy GDGTs dominated the intact polar lipid pool

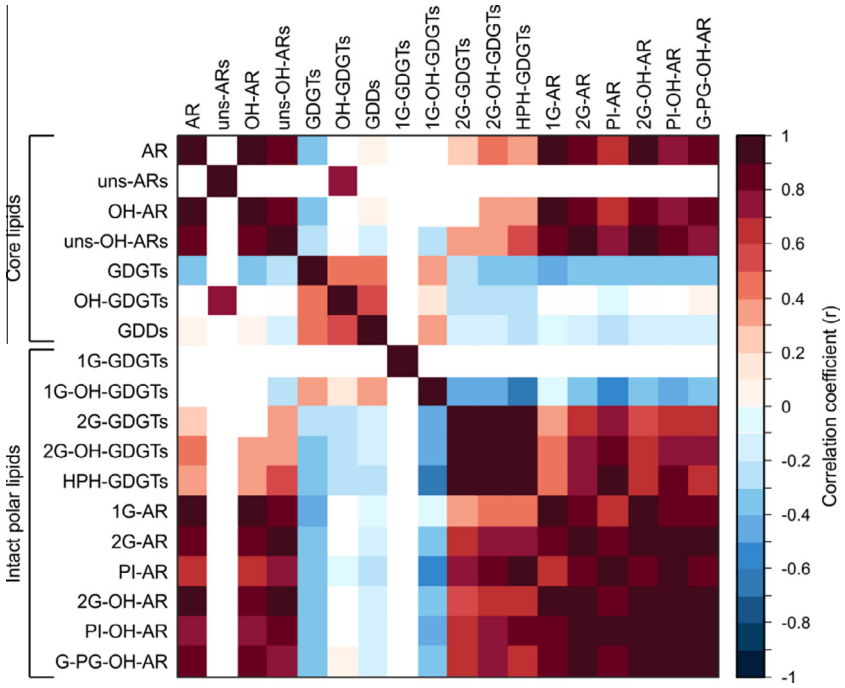

Fig. 9. Linear correlation coefficients ($p < 0.05$) calculated from relative abundances of core and intact polar lipids in Orca Basin sediments. Lipid nomenclature as described in Fig. 7.

(Fig. 7). These lipids are typical for planktonic *Thaumarchaeota* (Schouten et al., 2008; Elling et al., 2014) but may also be produced in significant amounts by benthic archaea, e.g., heterotrophs (Biddle et al., 2006; Lipp and Hinrichs, 2009), methanogens (Tornabene and Langworthy, 1979; Koga et al., 1993) and ANME-1 and ANME-2 methanotrophs (e.g., Rossel et al., 2008). Additionally, GDGTs are not known to be produced by extremely halophilic archaea (Kates, 1993). The relative abundances of intact polar GDGTs were not significantly correlated to the abundances of core and intact polar archaeols, suggesting different sources of GDGTs and archaeols. Given the high abundance of Marine Group I *Thaumarchaeota* 16S rRNA gene sequences that were possibly preserved (cf. Section 4.4), preservation of water column-derived thaumarchaeal intact polar lipids (cf. *Sargassum* lipid preservation in Orca Basin; Harvey and Kennicutt, 1992; Kennicutt et al., 1992) in the anoxic brine may likewise contribute significant amounts of fossil intact polar GDGTs to the sedimentary lipid pool.

Intact polar diether lipids consisted of saturated archaeols and hydroxyarchaeols with glycosidic and phosphatidic headgroups, which have been found in cultivated methanogens, e.g., halophilic *Methanohalophilus mahii* (Koga et al., 1993), as well as uncultivated putatively methanotrophic archaea of the ANME-1, ANME-2 and ANME-3 clades (Rossel et al., 2008). Intact polar lipid diversity and relative abundance of archaeal diether lipids was highest at 50–55 cm sediment depth in the northern basin (72%, Fig. 7), potentially indicating high levels of methanogenic biomass and/or activity in this sample. This is consistent with high abundances of 16S rRNA gene sequences related to methylotrophic methanogens (Section 4.4).

The $\delta^{13}C$ values of GDGT-derived biphytanes (−17‰ to −21‰) resemble those of TOC (−20‰ to −21‰) and are therefore compatible with both a planktonic and a benthic heterotrophic archaeal source (Fig. 8; Hoefs et al., 1997; Biddle et al., 2006; Könneke et al., 2012). In contrast, *sn*-2-hydroxyarchaeol was highly depleted in ^{13}C in all samples ($\delta^{13}C$: −77‰ to −78‰). Although these values fall into the range commonly associated with archaeal methanotrophy (∼−60‰ to −130‰; Hinrichs et al., 1999; Pancost et al., 2000; Blumenberg et al., 2004; Niemann and Elvert, 2008), the lack of AOM activity precludes a predominantly methanotrophic source of these lipids. Indeed, rather depleted methanogen lipids (e.g., −53‰ to −92‰) have been observed in the culture of *Methanosarcina barkeri* grown with methanol and TMA as the primary substrates (Summons et al., 1998; Londry et al., 2008) and in *Methanococcoides burtonii* grown on TMA (Summons et al., 1998). Based on the lipid fractionation in *Methanosarcina barkeri* (Londry et al., 2008), methylotrophic methanogenesis from methanol or TMA would yield $\delta^{13}C$ values similar to those observed in Orca Basin. For example, using the *in situ* $\delta^{13}C$ values of TMA (−36‰ to −37‰, Fig. 3), methanogenesis from TMA would yield archaeol and hydroxyarchaeol $\delta^{13}C$ values of −49‰ to −79‰ (Fig. 8; Table S7). Likewise, methanogenesis from methanol would yield lipid $\delta^{13}C$ values of −28‰ to −74‰ assuming that methanol is derived from fermentation of TOC (i.e., $\delta^{13}C_{methanol} \sim \delta^{13}C_{TOC}$). Strongly ^{13}C-depleted lipids could also be derived from hydrogenotrophic methanogenesis (Fig. 8; Table S7), but the high abundance and activity of methylotrophic relative to hydrogenotrophic methanogens in Orca Basin sediments suggest that the ^{13}C-depleted lipids were derived predominantly from methylotrophic methanogens.

Monounsaturated *sn*-2-hydroxyarchaeol and the *sn*-3 isomer of hydroxyarchaeol showed similar ^{13}C depletion as *sn*-2-hydroxyarchaeol, indicating that they likely originated from the same methanogenic source. Archaeol was less depleted in ^{13}C than hydroxyarchaeol derivatives in all samples, indicating a mixture of methanogenic and other sources, e.g., heterotrophic halophiles. The strong ^{13}C-depletion of archaeol (−78‰) in the 50–55 cm sample in the northern basin indicates a dominance of the methanogenic signal over other archaeal sources, consistent with the highest relative abundances of *Methanohalophilus* sequences as well as core and intact polar hydroxyarchaeol at this depth. In contrast, monounsaturated archaeol was less depleted (−59‰) than archaeol (−78‰). This intermediate $\delta^{13}C$ value might reflect mixed sources of this lipid, as some methanogens as well as *Halobacteriales* are known to produce it (e.g., Nichols and Franzmann, 1992; Franzmann et al., 1992).

In conclusion, polyunsaturated core archaeols found in Orca Basin are potentially derived from extremely halophilic *Halobacteriales*-like archaea. In contrast, polyunsaturated core hydroxyarchaeols, strongly ^{13}C-depleted hydroxyarchaeols as well as intact polar archaeols and hydroxyarchaeols indicate that the archaeal community in the sediments of Orca Basin is primarily composed of methylotrophic methanogenic archaea and to a lesser extent of methanotrophic archaea.

5. CONCLUSIONS

Significant amounts of methane were observed in hypersaline sediments from southern and northern Orca Basin. Although previous biogeochemical investigations suggested a potential of methylated compounds as methanogenic substrates in hypersaline environments, the formation of methane in deep-sea hypersaline basins remained largely unconstrained. In this study, multiple lines of evidence suggested that methylotrophic methanogenesis is the major source of methane in Orca Basin sediments:

(1) Highly depleted $\delta^{13}C$ values of methane in the range of −77‰ to −89‰ strongly supported a biogenic origin of methane in Orca Basin.
(2) Hydrogenotrophic and acetoclastic methanogenesis were unlikely to occur in Orca Basin due to competitive inhibition by sulfate reducers in the presence of abundant sulfate, low concentrations of H_2 and no detectable acetate. In contrast, methylated substrates and their precursors were highly abundant relative to the non-hypersaline reference site, suggesting that these substrates could potentially fuel methane production in the hypersaline sediments of Orca Basin.
(3) Thermodynamic calculations demonstrated that methylotrophic methanogenesis was more favorable than hydrogenotrophic and acetoclastic methanogenesis under *in situ* conditions. High energy yields from methylotrophic methanogenesis could facilitate the survival of halophilic methanogens, as halophiles require more energy to maintain an osmotically balanced and functional cytoplasm.
(4) Stable isotope tracer experiments with different ^{13}C-labeled substrates indicated ^{13}C incorporation into methane only from methanol in sediments from northern Orca Basin. In addition, methanogenesis from ^{14}C-labeled methylamine but not from bicarbonate or acetate was detected in shallow sediments of the northern basin, attesting that methylotrophic methanogenesis was the dominant methanogenic pathway.
(5) 16S rRNA gene sequences related to obligately halophilic methylotrophic methanogens of the genus *Methanohalophilus* were abundant in the clone library sequences constructed from extracted DNA and dominated archaeal 16S rRNA gene sequence libraries in the subsurface of the northern basin. High abundances of strongly ^{13}C-depleted lipid biomarkers of putative methanogenic origin, e.g., intact polar and polyunsaturated hydroxyarchaeols, were consistent with the occurrence of methylotrophic methanogens.

ACKNOWLEDGEMENTS

We thank associate editor Tom McCollom and two anonymous reviewers for providing comments that improved an earlier version of this manuscript. We gratefully acknowledge the captain, crew and participating scientists of RV *Atlantis* cruise AT18-2. The cruise and the sampling program in the deep Gulf of Mexico and Orca Basin were supported by NSF Emerging Frontiers/Microbial Observatories and Microbial Interactions and Processes (Collaborative Research: A Microbial Observatory examining Microbial Abundance, Diversity, Associations, and Activity at Seafloor Brine Seeps. PIs: S. B. Joye, I. MacDonald and A. Teske; award number EF-0801741). V.B. Heuer, Y.-S. Lin and M.Y. Yoshinaga are thanked for supporting incubation experiments as well as biogeochemical and lipid analyses. We thank J. Wendt for supporting TOC analyses. The study was supported by the DFG through the Research Center/Excellence Cluster MARUM-Center for Marine Environmental Sciences. G.-C. Zhuang was sponsored by the Chinese Scholarship Council (CSC) and the Bremen International Graduate School for Marine Sciences (GLOMAR).

APPENDIX A. SUPPLEMENTARY DATA

Supplementary data associated with this article can be found, in the online version, at http://dx.doi.org/10.1016/j.gca.2016.05.005.

REFERENCES

Antunes A., Ngugi D. K. and Stingl U. (2011) Microbiology of the Red Sea (and other) deep-sea anoxic brine lakes. *Environ. Microbiol. Rep.* **3**, 416–433.

Avrahamov N., Antler G., Yechieli Y., Gavrieli I., Joye S., Saxton M., Turchyn A. and Sivan O. (2014) Anaerobic oxidation of methane by sulfate in hypersaline groundwater of the Dead Sea aquifer. *Geobiology* **12**, 511–528.

Biddle J. F., Lipp J. S., Lever M. A., Lloyd K. G., Sørensen K. B., Anderson R., Fredricks H. F., Elvert M., Kelly T. J., Schrag D. P., Sogin M. L., Brenchley J. E., Teske A., House C. H. and Hinrichs K.-U. (2006) Heterotrophic Archaea dominate sedi-

mentary subsurface ecosystems off Peru. *Proc. Natl. Acad. Sci. U.S.A.* **103**, 3846–3851.

Blumenberg M., Seifert R., Reitner J., Pape T. and Michaelis W. (2004) Membrane lipid patterns typify distinct anaerobic methanotrophic consortia. *Proc. Natl. Acad. Sci. U.S.A.* **101**, 11111–11116.

Boetius A. and Joye S. B. (2009) Thriving in salt. *Science* **324**, 1523–1525.

Bowles M. W., Samarkin V. A. and Joye S. B. (2011) Improved measurement of microbial activity in deep-sea sediments at in situ pressure and methane concentration. *Limnol. Oceanogr.-Methods* **9**, 499–506.

Bradley A. S., Hayes J. M. and Summons R. E. (2009) Extraordinary ^{13}C enrichment of diether lipids at the Lost City Hydrothermal Field indicates a carbon-limited ecosystem. *Geochim. Cosmochim. Acta* **73**, 102–118.

Charlou J., Donval J., Zitter T., Roy N., Jean-Baptiste P., Foucher J. and Woodside J. (2003) Evidence of methane venting and geochemistry of brines on mud volcanoes of the eastern Mediterranean Sea. *Deep-Sea Res. I* **50**, 941–958.

Cline J. D. (1969) Spectrophotometric determination of hydrogen sulfide in natural waters. *Limnol. Oceanogr.* **14**, 454–458.

Conrad R. (2005) Quantification of methanogenic pathways using stable carbon isotopic signatures: a review and a proposal. *Org. Geochem.* **36**, 739–752.

Corinaldesi C., Barucca M., Luna G. M. and Dell'Anno A. (2011) Preservation, origin and genetic imprint of extracellular DNA in permanently anoxic deep-sea sediments. *Mol. Ecol.* **20**, 642–654.

Crozier T. E. and Yamamoto S. (1974) Solubility of hydrogen in water, sea water, and sodium chloride solutions. *J. Chem. Eng. Data* **19**, 242–244.

Dawson K. S., Freeman K. H. and Macalady J. L. (2012) Molecular characterization of core lipids from halophilic archaea grown under different salinity conditions. *Org. Geochem.* **48**, 1–8.

Donnelly M. and Dagley S. (1980) Production of methanol from aromatic acids by *Pseudomonas putida*. *J. Bacteriol.* **142**, 916–924.

Elling F. J., Könneke M., Lipp J. S., Becker K. W., Gagen E. J. and Hinrichs K.-U. (2014) Effects of growth phase on the membrane lipid composition of the thaumarchaeon *Nitrosopumilus maritimus* and their implications for archaeal lipid distributions in the marine environment. *Geochim. Cosmochim. Acta* **141**, 579–597.

Ertefai T. F., Heuer V. B., Prieto-Mollar X., Vogt C., Sylva S. P., Seewald J. and Hinrichs K.-U. (2010) The biogeochemistry of sorbed methane in marine sediments. *Geochim. Cosmochim. Acta* **75**, 6033–6048.

Faber E., Botz R., Poggenburg J., Schmidt M., Stoffers P. and Hartmann M. (1998) Methane in Red Sea brines. *Org. Geochem.* **29**, 363–379.

Franzmann P., Springer N., Ludwig W., Conway de Macario E. and Rohde M. (1992) A methanogenic archaeon from Ace Lake, Antarctica: *Methanococcoides burtonii* sp. nov. *Syst. Appl. Microbiol.* **15**, 573–581.

Gelwicks J. T., Risatti J. B. and Hayes J. (1989) Carbon isotope effects associated with autotrophic acetogenesis. *Org. Geochem.* **14**, 441–446.

Gibson J. A., Miller M. R., Davies N. W., Neill G. P., Nichols D. S. and Volkman J. K. (2005) Unsaturated diether lipids in the psychrotrophic archaeon *Halorubrum lacusprofundi*. *Syst. Appl. Microbiol.* **28**, 19–26.

Golyshina O. V., Lünsdorf H., Kublanov I. V., Goldenstein N. I., Hinrichs K.-U. and Golyshin P. N. (2016) The novel extremely acidophilic, cell-wall-deficient archaeon *Cuniculiplasma divulgatum* gen. nov., sp. nov. represents a new family, *Cuniculiplasmataceae* fam. nov., of the order *Thermoplasmatales*. *Int. J. Syst. Evol. Microbiol.* **66**, 332–340.

Harvey H. R. and Kennicutt, II, M. C. (1992) Selective alteration of *Sargassum* lipids in anoxic sediments of the Orca Basin. *Org. Geochem.* **18**, 181–187.

Heuer V., Elvert M., Tille S., Krummen M., Prieto Mollar X., Hmelo L. R. and Hinrichs K.-U. (2006) Online $\delta^{13}C$ analysis of volatile fatty acids in sediment/porewater systems by liquid chromatography-isotope ratio-mass spectrometry. *Limnol. Oceanogr. Methods* **4**, 346–357.

Hinrichs K.-U., Hayes J. M., Sylva S. P., Brewer P. G. and DeLong E. F. (1999) Methane-consuming archaebacteria in marine sediments. *Nature* **398**, 802–805.

Hoefs M. J. L., Schouten S., De Leeuw J. W., King L. L., Wakeham S. G. and Sinninghe Damsté J. S. (1997) Ether lipids of planktonic archaea in the marine water column. *Appl. Environ. Microbiol.* **63**, 3090–3095.

Hoehler T. M. (2004) Biological energy requirements as quantitative boundary conditions for life in the subsurface. *Geobiology* **2**, 205–215.

Hoehler T. M., Alperin M. J., Albert D. B. and Martens C. S. (1998) Thermodynamic control on hydrogen concentrations in anoxic sediments. *Geochim. Cosmochim. Acta* **62**, 1745–1756.

Huber H., Hohn M. J., Rachel R., Fuchs T., Wimmer V. C. and Stetter K. O. (2002) A new phylum of archaea represented by a nanosized hyperthermophilic symbiont. *Nature* **417**, 63–67.

Joye S. B., Boetius A., Orcutt B. N., Montoya J. P., Schulz H. N., Erickson M. J. and Lugo S. K. (2004) The anaerobic oxidation of methane and sulfate reduction in sediments from Gulf of Mexico cold seeps. *Chem. Geol.* **205**, 219–238.

Joye S. B., MacDonald I. R., Montoya J. P. and Peccini M. (2005) Geophysical and geochemical signatures of Gulf of Mexico seafloor brines. *Biogeosciences* **2**, 295–309.

Joye S. B., Samarkin V. A., MacDonald I. R., Hinrichs K.-U., Elvert M., Teske A. P., Lloyd K. G., Lever M. A., Montoya J. P. and Meile C. D. (2009) Metabolic variability in seafloor brines revealed by carbon and sulphur dynamics. *Nat. Geosci.* **2**, 349–354.

Joye S. B., Bowles M. W., Samarkin V. A., Hunter K. S. and Niemann H. (2010) Biogeochemical signatures and microbial activity of different cold-seep habitats along the Gulf of Mexico deep slope. *Deep-Sea Res. II* **57**, 1990–2001.

Kamanda Ngugi. D., Blom J., Alam I., Rashid M., Ba-Alawi W., Zhang G., Hikmawan T., Guan Y., Antunes A., Siam R., El Dorry H., Bajic V. and Stingl U. (2015) Comparative genomics reveals adaptations of a halotolerant thaumarchaeon in the interfaces of brine pools in the Red Sea. *ISME J.* **9**, 396–411.

Kates M. (1993) Biology of halophilic bacteria, Part II. *Experientia* **49**, 1027–1036.

Keller M. D., Bellows W. K. and Guillard R. R. (1989) Dimethyl sulfide production in marine phytoplankton. In *Biogenic Sulfur in the Environment* (eds. E. S. Saltzman and W. J. Cooper). American Chemical Society, Washington, DC, pp. 167–182.

Kelley C. A., Poole J. A., Tazaz A. M., Chanton J. P. and Bebout B. M. (2012) Substrate limitation for methanogenesis in hypersaline environments. *Astrobiology* **12**, 89–97.

Kennicutt M., Macko S. A., Harvey H. R. and Bidigare R. R. (1992) Preservation of *Sargassum* under anoxic conditions: molecular and isotopic evidence. In *Organic matter: Productivity, Accumulation, and Preservation in Recent and Ancient Sediments* (eds. J. F. Farrington and J. K. Whelan). Columbia University Press, New York, pp. 123–141.

Kiene R. P., Oremland R. S., Catena A., Miller L. G. and Capone D. G. (1986) Metabolism of reduced methylated sulfur compounds in anaerobic sediments and by a pure culture of

an estuarine methanogen. *Appl. Environ. Microbiol.* **52**, 1037–1045.

King G., Klug M. and Lovley D. (1983) Metabolism of acetate, methanol, and methylated amines in intertidal sediments of lowes cove, maine. *Appl. Environ. Microbiol.* **45**, 1848–1853.

Koga Y. and Morii H. (2005) Recent advances in structural research on ether lipids from archaea including comparative and physiological aspects. *Biosci. Biotechnol. Biochem.* **69**, 2019–2034.

Koga Y., Nishihara M., Morii H. and Akagawa-Matsushita M. (1993) Ether polar lipids of methanogenic bacteria: structures, comparative aspects, and biosyntheses. *Microbiol. Rev.* **57**, 164–182.

Könneke M., Lipp J. S. and Hinrichs K.-U. (2012) Carbon isotope fractionation by the marine ammonia-oxidizing archaeon *Nitrosopumilus maritimus*. *Org. Geochem.* **48**, 21–24.

Krzycki J., Kenealy W., DeNiro M. and Zeikus J. (1987) Stable carbon isotope fractionation by *Methanosarcina barkeri* during methanogenesis from acetate, methanol, or carbon dioxide-hydrogen. *Appl. Environ. Microbiol.* **53**, 2597–2599.

Kulp T., Han S., Saltikov C., Lanoil B., Zargar K. and Oremland R. (2007) Effects of imposed salinity gradients on dissimilatory arsenate reduction, sulfate reduction, and other microbial processes in sediments from two California soda lakes. *Appl. Environ. Microbiol.* **73**, 5130–5137.

Lazar C. S., Parkes R. J., Cragg B. A., L'Haridon S. and Toffin L. (2011) Methanogenic diversity and activity in hypersaline sediments of the centre of the Napoli mud volcano, Eastern Mediterranean Sea. *Environ. Microbiol.* **13**, 2078–2091.

Lin Y.-S., Heuer V. B., Goldhammer T., Kellermann M. Y., Zabel M. and Hinrichs K.-U. (2012) Towards constraining H_2 concentration in subseafloor sediment: a proposal for combined analysis by two distinct approaches. *Geochim. Cosmochim. Acta* **77**, 186–201.

Lipp J. S. and Hinrichs K.-U. (2009) Structural diversity and fate of intact polar lipids in marine sediments. *Geochim. Cosmochim. Acta* **73**, 6816–6833.

Liu Y., Boone D. R. and Choy C. (1990) *Methanohalophilus oregonense* sp. nov., a methylotrophic methanogen from an alkaline, saline aquifer. *Int. J. Syst. Bacteriol.* **40**, 111–116.

Liu X.-L., Lipp J. S. and Hinrichs K.-U. (2011) Distribution of intact and core GDGTs in marine sediments. *Org. Geochem.* **42**, 368–375.

Liu X.-L., Lipp J. S., Simpson J. H., Lin Y.-S., Summons R. E. and Hinrichs K.-U. (2012a) Mono- and dihydroxyl glycerol dibiphytanyl glycerol tetraethers in marine sediments: Identification of both core and intact polar lipid forms. *Geochim. Cosmochim. Acta* **89**, 102–115.

Liu X.-L., Lipp J. S., Schröder J. M., Summons R. E. and Hinrichs K.-U. (2012b) Isoprenoid glycerol dialkanol diethers: a series of novel archaeal lipids in marine sediments. *Org. Geochem.* **43**, 50–55.

Londry K. L., Dawson K. G., Grover H. D., Summons R. E. and Bradley A. S. (2008) Stable carbon isotope fractionation between substrates and products of *Methanosarcina barkeri*. *Org. Geochem.* **39**, 608–621.

Ludwig W., Strunk O., Westram R., Richter L., Meier H., Buchner A., Lai T., Steppi S., Jobb G. and Förster W. (2004) ARB: a software environment for sequence data. *Nucl. Acids Res.* **32**, 1363–1371.

Mancinelli R., Fahlen T., Landheim R. and Klovstad M. (2004) Brines and evaporites: analogs for Martian life. *Adv. Space Res.* **33**, 1244–1246.

Marvin-DiPasquale M., Oren A., Cohen Y. and Oremland R. S. (1999) Radiotracer studies of bacterial methanogenesis in sediments from the Dead Sea and Solar Lake (Sinai). In *Microbiology and Biogeochemistry of Hypersaline Environments* (ed. A. Oren). CRC Press, Boca Raton, pp. 149–160.

McGenity T. (2010) *Methanogens and Methanogenesis in Hypersaline Environments. Handbook of Hydrocarbon and Lipid Microbiology*. Springer, pp. 665–680.

Mook W., Bommerson J. and Staverman W. (1974) Carbon isotope fractionation between dissolved bicarbonate and gaseous carbon dioxide. *Earth Planet. Sci. Lett.* **22**, 169–176.

Nauhaus K., Treude T., Boetius A. and Krüger M. (2005) Environmental regulation of the anaerobic oxidation of methane: a comparison of ANME-I and ANME-II communities. *Environ. Microbiol.* **7**, 98–106.

Nichols P. D. and Franzmann P. D. (1992) Unsaturated diether phospholipids in the Antartic methanogen *Methanococcoides burtonii*. *FEMS Microbiol. Lett.* **98**, 205–208.

Nichols D. S., Miller M. R., Davies N. W., Goodchild A., Raftery M. and Cavicchioli R. (2004) Cold adaptation in the Antarctic archaeon *Methanococcoides burtonii* involves membrane lipid unsaturation. *J. Bacteriol.* **186**, 8508–8515.

Niemann H. and Elvert M. (2008) Diagnostic lipid biomarker and stable carbon isotope signatures of microbial communities mediating the anaerobic oxidation of methane with sulphate. *Org. Geochem.* **39**, 1668–1677.

Northam M. A., Curry D. J., Scalan R. S. and Parker P. L. (1981) Stable carbon isotope ratio variations of organic matter in Orca Basin sediments. *Geochim. Cosmochim. Acta* **45**, 257–260.

Ollivier B., Caumette P., Garcia J.-L. and Mah R. (1994) Anaerobic bacteria from hypersaline environments. *Microbiol. Rev.* **58**, 27–38.

Oremland R. S. and Miller L. M. (1993) *Biogeochemistry of Natural Gases in Three Alkaline, Permanently Stratified (meromictic) Lakes*. United States Geological Survey, Professional Paper, United States, pp. 439–452.

Oremland R. S. and Polcin S. (1982) Methanogenesis and sulfate reduction: competitive and noncompetitive substrates in estuarine sediments. *Appl. Environ. Microbiol.* **44**, 1270–1276.

Oremland R. S., Marsh L. M. and DesMarais D. J. (1982a) Methanogenesis in Big Soda Lake, Nevada: an alkaline, moderately hypersaline desert lake. *Appl. Environ. Microbiol.* **43**, 462–468.

Oremland R. S., Marsh L. M. and Polcin S. (1982b) Methane production and simultaneous sulphate reduction in anoxic, salt marsh sediments. *Nature* **296**, 143–145.

Oremland R. S., Kiene R. P., Mathrani I., Whiticar M. J. and Boone D. R. (1989) Description of an estuarine methylotrophic methanogen which grows on dimethyl sulfide. *Appl. Environ. Microbiol.* **55**, 994–1002.

Oremland R. S., Miller L. G., Colbertson C. W., Robinson S., Smith R. L., Lovley D., Whiticar M. J., King G. M., Kiene R. P. and Iversen N. (1993) Aspects of the biogeochemistry of methane in Mono Lake and the Mono Basin of California. *Biogeochem. Glob. Chang. Springer*, 704–741.

Oren A. (1990) Formation and breakdown of glycine betaine and trimethylamine in hypersaline environments. *Antonie Van Leeuwenhoek* **58**, 291–298.

Oren A. (1999) Bioenergetic aspects of halophilism. *Microbiol. Mol. Biol. Rev.* **63**, 334–348.

Oren A. (2008) Microbial life at high salt concentrations: phylogenetic and metabolic diversity. *Saline Syst.* **4**, 13.

Orphan V., Jahnke L., Embaye T., Turk K., Pernthaler A., Summons R. E. and Des Marais. D. (2008) Characterization and spatial distribution of methanogens and methanogenic biosignatures in hypersaline microbial mats of Baja California. *Geobiology* **6**, 376–393.

Pancost R. D., Damsté Sinninghe J. S., de Lint S., van der Maarel M. J. E. C., Gottschal J. C. and The Medinaut Shipboard

Scientific Party (2000) Biomarker evidence for widespread anaerobic methane oxidation in Mediterranean sediments by a consortium of methanogenic archaea and bacteria. *Appl. Environ. Microbiol.* **66**, 1126–1132.

Paterek J. R. and Smith P. H. (1988) *Methanohalophilus mahii* gen. nov., sp. nov., a methylotrophic halophilic methanogen. *Int. J. Syst. Bacteriol.* **38**, 122–123.

Penger J., Conrad R. and Blaser M. (2012) Stable carbon isotope fractionation by methylotrophic methanogenic archaea. *Appl. Environ. Microbiol.* **78**, 7596–7602.

Penning H., Claus P., Casper P. and Conrad R. (2006) Carbon isotope fractionation during acetoclastic methanogenesis by *Methanosaeta concilii* in culture and a lake sediment. *Appl. Environ. Microbiol.* **72**, 5648–5652.

Pilcher R. S. and Blumstein R. D. (2007) Brine volume and salt dissolution rates in Orca Basin, northeast Gulf of Mexico. *AAPG Bull.* **91**, 823–833.

Pruesse E., Peplies J. and Glöckner F. O. (2012) SINA: accurate high-throughput multiple sequence alignment of ribosomal RNA genes. *Bioinformatics* **28**, 1823–1829.

Qiu D. F., Games M. P., Xiao X. Y., Games D. E. and Walton T. J. (1998) Application of high-performance liquid chromatography/electrospray mass spectrometry for the characterization of membrane lipids in the haloalkaliphilic archaebacterium *Natronobacterium magadii*. *Rapid Commun. Mass Spectrom.* **12**, 939–946.

Quast C., Pruesse E., Yilmaz P., Gerken J., Schweer T., Yarza P., Peplies J. and Glöckner F. O. (2012) The SILVA ribosomal RNA gene database project: improved data processing and web-based tools. *Nucl. Acids Res.*, gks1219.

Roberts M. F. (2005) Organic compatible solutes of halotolerant and halophilic microorganisms. *Saline Syst.* **1**, 1–30.

Rosenfeld W. D. and Silverman S. R. (1959) Carbon isotope fractionation in bacterial production of methane. *Science* **130**, 1658–1659.

Rossel P. E., Lipp J. S., Fredricks H. F., Arnds J., Boetius A., Elvert M. and Hinrichs K.-U. (2008) Intact polar lipids of anaerobic methanotrophic archaea and associated bacteria. *Org. Geochem.* **39**, 992–999.

Rossel P. E., Elvert M., Ramette A., Boetius A. and Hinrichs K.-U. (2011) Factors controlling the distribution of anaerobic methanotrophic communities in marine environments: evidence from intact polar membrane lipids. *Geochim. Cosmochim. Acta* **75**, 164–184.

Sackett W. M., Brooks J., Bernard B., Schwab C., Chung H. and Parker R. (1979) A carbon inventory for Orca Basin brines and sediments. *Earth Planet. Sci. Lett.* **44**, 73–81.

Schijf J. (2007) Alkali elements (Na, K, Rb) and alkaline earth elements (Mg, Ca, Sr, Ba) in the anoxic brine of Orca Basin, northern Gulf of Mexico. *Chem. Geol.* **243**, 255–274.

Schink B. and Stams A. J. (2006) Syntrophism among prokaryotes. In *The Prokaryotes* (eds. E. Rosenberg, E. F. DeLong, S. Lory, E. Stackebrandt and F. Thompson). Springer, Berlin, pp. 471–493.

Schink B. and Zeikus J. (1980) Microbial methanol formation: a major end product of pectin metabolism. *Curr. Microbiol.* **4**, 387–389.

Schouten S., Hopmans E. C., Pancost R. D. and Sinninghe Damsté J. S. (2000) Widespread occurrence of structurally diverse tetraether membrane lipids: evidence for the ubiquitous presence of low-temperature relatives of hyperthermophiles. *Proc. Natl. Acad. Sci. U.S.A.* **97**, 14421–14426.

Schouten S., Hopmans E. C., Baas M., Boumann H., Standfest S., Könneke M., Stahl D. A. and Sinninghe Damsté J. S. (2008) Intact membrane lipids of "*Candidatus* Nitrosopumilus maritimus", a cultivated representative of the cosmopolitan mesophilic group I crenarchaeota. *Appl. Environ. Microbiol.* **74**, 2433–2440.

Schulz S., Matsuyama H. and Conrad R. (1997) Temperature dependence of methane production from different precursors in a profundal sediment (Lake Constance). *FEMS Microbiol. Ecol.* **22**, 207–213.

Shokes R. F., Trabant P. K., Presley B. J. and Reid D. F. (1977) Anoxic, hypersaline basin in the northern Gulf of Mexico. *Science* **196**, 1443–1446.

Smith J. M., Green S. J., Kelley C. A., Prufert-Bebout L. and Bebout B. M. (2008) Shifts in methanogen community structure and function associated with long-term manipulation of sulfate and salinity in a hypersaline microbial mat. *Environ. Microbiol.* **10**, 386–394.

Sprott G., Ekiel I. and Dicaire C. (1990) Novel, acid-labile, hydroxydiether lipid cores in methanogenic bacteria. *J. Biol. Chem.* **265**, 13735–13740.

Stumm W. and Morgan J. J. (1981) *Aquatic chemistry: an introduction emphasizing chemical equilibria in natural waters*. Wiley, Toronto.

Sturt H. F., Summons R. E., Smith K., Elvert M. and Hinrichs K.-U. (2004) Intact polar membrane lipids in prokaryotes and sediments deciphered by high-performance liquid chromatography/electrospray ionization multistage mass spectrometry-new biomarkers for biogeochemistry and microbial ecology. *Rapid Commun. Mass Spectrom.* **18**, 617–628.

Summons R. E., Franzmann P. D. and Nichols P. D. (1998) Carbon isotopic fractionation associated with methylotrophic methanogenesis. *Org. Geochem.* **28**, 465–475.

Teske A., Hinrichs K.-U., Edgcomb V., de Vera Gomez A., Kysela D., Sylva S. P., Sogin M. L. and Jannasch H. W. (2002) Microbial diversity of hydrothermal sediments in the Guaymas Basin: evidence for anaerobic methanotrophic communities. *Appl. Environ. Microbiol.* **68**, 1994–2007.

Tornabene T. G. and Langworthy T. A. (1979) Diphytanyl and dibiphytanyl glycerol ether lipids of methanogenic archaebacteria. *Science* **203**, 51–53.

Tribovillard N., Bout-Roumazeilles V., Algeo T., Lyons T. W., Sionneau T., Montero-Serrano J. C., Riboulleau A. and Baudin F. (2008) Paleodepositional conditions in the Orca Basin as inferred from organic matter and trace metal contents. *Mar. Geol.* **254**, 62–72.

Tribovillard N., Bout-Roumazeilles V., Sionneau T., Serrano J. C. M., Riboulleau A. and Baudin F. (2009) Does a strong pycnocline impact organic-matter preservation and accumulation in an anoxic setting? The case of the Orca Basin, Gulf of Mexico. *C. R. Geosci.* **341**, 1–9.

Turich C. and Freeman K. H. (2011) Archaeal lipids record paleosalinity in hypersaline systems. *Org. Geochem.* **42**, 1147–1157.

Turich C., Freeman K. H., Bruns M. A., Conte M., Jones A. D. and Wakeham S. G. (2007) Lipids of marine Archaea: patterns and provenance in the water-column and sediments. *Geochim. Cosmochim. Acta* **71**, 3272–3291.

Valentine D. L., Chidthaisong A., Rice A., Reeburgh W. S. and Tyler S. C. (2004) Carbon and hydrogen isotope fractionation by moderately thermophilic methanogens. *Geochim. Cosmochim. Acta* **68**, 1571–1590.

van der Maarel M. J. E. C. and Hansen T. A. (1997) Dimethylsulfoniopropionate in anoxic intertidal sediments: a precursor of methanogenesis via dimethyl sulfide, methanethiol, and methiolpropionate. *Mar. Geol.* **137**, 5–12.

van der Wielen P. W., Bolhuis H., Borin S., Daffonchio D., Corselli C., Giuliano L., D'Auria G., de Lange G. J., Huebner A. and Varnavas S. P. (2005) The enigma of prokaryotic life in deep hypersaline anoxic basins. *Science* **307**, 121–123.

Wagman D. D., Evans W. H., Parker V. B., Schumm R. H. and Halow I. (1982) *The NBS Tables of Chemical Thermodynamic Properties. Selected Values for Inorganic and C1 and C2 Organic Substances in SI Units*. American Chemical Society and the American Institute of Physics for the National Bureau of Standards, Washington, DC.

Wakeham S. G., Amann R., Freeman K. H., Hopmans E. C., Jørgensen B. B., Putnam I. F., Schouten S., Sinninghe Damsté J. S., Talbot H. M. and Woebken D. (2007) Microbial ecology of the stratified water column of the Black Sea as revealed by a comprehensive biomarker study. *Org. Geochem.* **38**, 2070–2097.

Wang X.-C. and Lee C. (1994) Sources and distribution of aliphatic amines in salt marsh sediment. *Org. Geochem.* **22**, 1005–1021.

Wang X.-C. and Lee C. (1995) Decomposition of aliphatic amines and amino acids in anoxic salt marsh sediment. *Geochim. Cosmochim. Acta* **59**, 1787–1797.

Wegener G., Bausch M., Holler T., Thang N. M., Prieto M. X., Kellermann M. Y., Hinrichs K.-U. and Boetius A. (2012) Assessing sub-seafloor microbial activity by combined stable isotope probing with deuterated water and ^{13}C-bicarbonate. *Environ. Microbiol.* **14**, 1517–1527.

Whiticar M. J. (1999) Carbon and hydrogen isotope systematics of bacterial formation and oxidation of methane. *Chem. Geol.* **161**, 291–314.

Whiticar M. J., Faber E. and Schoell M. (1986) Biogenic methane formation in marine and freshwater environments: CO_2 reduction vs. acetate fermentation-isotope evidence. *Geochim. Cosmochim. Acta* **50**, 693–709.

Wiesenburg D. A., Brooks J. M. and Bernard B. B. (1985) Biogenic hydrocarbon gases and sulfate reduction in the Orca Basin brine. *Geochim. Cosmochim. Acta* **49**, 2069–2080.

Zeikus J. and Winfrey M. (1976) Temperature limitation of methanogenesis in aquatic sediments. *Appl. Environ. Microbiol.* **31**, 99–107.

Zhilina T. N. and Zavarzin G. A. (1990) Extremely halophilic, methylotrophic, anaerobic bacteria. *FEMS Microbiol. Lett.* **87**, 315–322.

Zhu C., Lipp J. S., Wörmer L., Becker K. W., Schröder J. and Hinrichs K.-U. (2013) Comprehensive glycerol ether lipid fingerprints through a novel reversed phase liquid chromatography–mass spectrometry protocol. *Org. Geochem.* **65**, 53–62.

Zhu C., Wakeham S. G., Elling F. J., Basse A., Mollenhauer G., Versteegh G. J., Könneke M. and Hinrichs K. U. (2016) Stratification of archaeal membrane lipids in the ocean and implications for adaptation and chemotaxonomy of planktonic archaea. *Environ. Microbiol.*. http://dx.doi.org/10.1111/1462-2920.13289.

Zhuang G.-C. (2014) *Methylotrophic Methanogenesis and Potential Methylated Substrates in Marine Sediment* Ph. D. thesis. Department of Geosciences, University of Bremen.

Zhuang G.-C., Yang G.-P., Yu J. and Gao Y. (2011) Production of DMS and DMSP in different physiological stages and salinity conditions in two marine algae. *Chin. J. Oceanol. Limnol.* **29**, 369–377.

Zhuang G.-C., Lin Y.-S., Elvert M., Heuer V. B. and Hinrichs K.-U. (2014) Gas chromatographic analysis of methanol and ethanol in marine sediment pore waters: validation and implementation of three pretreatment techniques. *Mar. Chem.* **160**, 82–90.

Associate editor: Thomas McCollom